NAVAL POSTGRADUATE SCHOOL

MONTEREY, CALIFORNIA

THESIS

LONG-ENDURANCE MARITIME SURVEILLANCE WITH OCEAN GLIDER NETWORKS

by

Bradley J. Nott

September 2015

Thesis Advisor: John E. Joseph
Second Reader: Tetyana Margolina

Approved for public release; distribution is unlimited

THIS PAGE INTENTIONALLY LEFT BLANK

REPORT DOCUMENTATION PAGE	*Form Approved OMB No. 0704–0188*

1. AGENCY USE ONLY	**2. REPORT DATE** September 2015	**3. REPORT TYPE AND DATES COVERED** Master's thesis

4. TITLE AND SUBTITLE
LONG-ENDURANCE MARITIME SURVEILLANCE
WITH OCEAN GLIDER NETWORKS

5. FUNDING NUMBERS

6. AUTHOR(S) Nott, Bradley J.

7. PERFORMING ORGANIZATION NAME(S) AND ADDRESS(ES)
Naval Postgraduate School
Monterey, CA 93943–5000

8. PERFORMING ORGANIZATION REPORT NUMBER

9. SPONSORING /MONITORING AGENCY NAME(S) AND ADDRESS(ES)
N/A

10. SPONSORING / MONITORING AGENCY REPORT NUMBER

11. SUPPLEMENTARY NOTES The views expressed in this thesis are those of the author and do not reflect the official policy or position of the Department of Defense or the U.S. Government. IRB Protocol number ____N/A____.

12a. DISTRIBUTION / AVAILABILITY STATEMENT Approved for public release; distribution is unlimited	**12b. DISTRIBUTION CODE** A

13. ABSTRACT (maximum 200 words)

This study examines the integration of ocean glider Unmanned Surface Vehicles (USVs) and Unmanned Undersea Vehicles (UUVs) in support of wide-area oceanographic and acoustic sampling. These collaborative systems could enable the U.S. Navy to conduct multi-month unmanned maritime surveillance. Optimal sensor position in the water column and persistence are critical requirements to reduce surface expressions of such a network. An experiment was conducted in Monterey Bay to evaluate underwater gliders as mobile passive acoustic sensing platforms. Acoustic propagation modeling was used to plan experiment geometry, predict transmission loss (TL), and estimate acoustic communications performance with a USV. A medium frequency acoustic source was deployed at a range of 5.5 km from a receiver on board a glider conducting a 1000 m dive to demonstrate that a glider can adapt to the local environment to exploit more reliable propagation paths. Results demonstrate that gliders are effective mobile platforms to support persistent acoustic sensing. The glider received transmitted signals at levels in close agreement with TL predictions. Signals were received while the glider was in motion, and reception improved during a quiet deep loiter. Given the depths, ranges, and environmental conditions studied, research and modeling suggest sufficient acoustic communication performance to promote connectivity of the proposed network.

14. SUBJECT TERMS Acoustics, Ocean gliders, long-endurance, maritime surveillance, unmanned systems, oceanographic sampling, passive acoustics, acoustic communications	**15. NUMBER OF PAGES** 87
	16. PRICE CODE

17. SECURITY CLASSIFICATION OF REPORT	**18. SECURITY CLASSIFICATION OF THIS PAGE**	**19. SECURITY CLASSIFICATION OF ABSTRACT**	**20. LIMITATION OF ABSTRACT**
Unclassified	Unclassified	Unclassified	UU

NSN 7540–01–280–5500 Standard Form 298 (Rev. 2–89)
Prescribed by ANSI Std. 239–18

THIS PAGE INTENTIONALLY LEFT BLANK

Approved for public release; distribution is unlimited

LONG-ENDURANCE MARITIME SURVEILLANCE WITH OCEAN GLIDER NETWORKS

Bradley J. Nott
Lieutenant, United States Navy
B. A., University of California, Los Angeles, 2006

Submitted in partial fulfillment of the
requirements for the degree of

MASTER OF SCIENCE IN PHYSICAL OCEANOGRAPHY

from the

NAVAL POSTGRADUATE SCHOOL
September 2015

Approved by: John E. Joseph
Thesis Advisor

Tetyana Margolina
Second Reader

Peter Chu
Chair, Department of Oceanography

THIS PAGE INTENTIONALLY LEFT BLANK

ABSTRACT

This study examines the integration of ocean glider Unmanned Surface Vehicles (USVs) and Unmanned Undersea Vehicles (UUVs) in support of wide-area oceanographic and acoustic sampling. These collaborative systems could enable the U.S. Navy to conduct multi-month unmanned maritime surveillance. Optimal sensor position in the water column and persistence are critical requirements to reduce surface expressions of such a network. An experiment was conducted in Monterey Bay to evaluate underwater gliders as mobile passive acoustic sensing platforms. Acoustic propagation modeling was used to plan experiment geometry, predict transmission loss (TL), and estimate acoustic communications performance with a USV. A medium frequency acoustic source was deployed at a range of 5.5 km from a receiver on board a glider conducting a 1000 m dive to demonstrate that a glider can adapt to the local environment to exploit more reliable propagation paths. Results demonstrate that gliders are effective mobile platforms to support persistent acoustic sensing. The glider received transmitted signals at levels in close agreement with TL predictions. Signals were received while the glider was in motion, and reception improved during a quiet deep loiter. Given the depths, ranges, and environmental conditions studied, research and modeling suggest sufficient acoustic communication performance to promote connectivity of the proposed network.

THIS PAGE INTENTIONALLY LEFT BLANK

TABLE OF CONTENTS

LIST OF FIGURES

LIST OF ACRONYMS AND ABBREVIATIONS

A2/AD	anti-access/area-denial
ASW	Anti-Submarine Warfare
BA	Battlespace Awareness
C2	command and control
CTD	conductivity, temperature, and depth
DFE	Decision Feedback Equalizer
DI	directivity index
DT	detection threshold
FEC	Forward Error Correction
FFT	Fast-Fourier Transform
GDEM	U.S. Navy Generalized Digital Environmental Model
GPS	global positioning system
ISI	Intersymbol Interference
ISR	Intelligence, Surveillance, and Reconnaissance
LTSA	Long-Term Spectral Average
N2/N6	Deputy Chief of Naval Operations for Information Dominance
NL	noise level
NUWC	Naval Undersea Warfare Center
PSD	Power Spectral Density
RAP	reliable acoustic path
R/V	research vessel
SL	source level
SNR	signal-to-noise ratio
SSP	sound speed profile
TL	transmission loss
USV	unmanned surface vehicle
UUV	unmanned underwater vehicle
USGS	U.S. Geological Survey
WHOI	Woods Hole Oceanographic Institution

THIS PAGE INTENTIONALLY LEFT BLANK

ACKNOWLEDGMENTS

I could not have completed this work without the support and guidance of several important individuals. First and foremost, I would like to thank my amazing wife, Jenae, for her love and encouragement during my studies in Monterey. She has helped make these past two years the most fulfilling of my time in the Navy. I never could have imagined that my orders to graduate school would have such a lasting impact on my life. Jenae, you and your parents have welcomed me into your family and made my time on the Monterey peninsula unforgettable. I am truly blessed.

I would like to thank my advisor, John Joseph, for his assistance with the thesis topic, help with analysis of the experimental data, and detailed input throughout the thesis revision process.

Tetyana Margolina was instrumental as my second reader. She graciously provided the detailed ocean bottom-type information for model runs and frequently donated her personal time to help refine my research.

Chris Miller helped me improve my knowledge of digital signal processing and data analysis in MATLAB.

Doug Horner introduced me to essential concepts in the fields of unmanned systems and acoustic communications.

Finally, I would like to thank my parents. Throughout my life, my father has been instrumental in helping me discover my love for science, history, music, and aviation. My mother supported my hobbies while I was growing up, and has always encouraged my creative efforts. I could not have accomplished what I have in my life without their love and encouragement.

THIS PAGE INTENTIONALLY LEFT BLANK

I. INTRODUCTION

The long-endurance of the autonomous underwater glider platform makes it an excellent candidate to support a mobile undersea acoustic cueing system. Such systems could enable the U.S. Navy to conduct persistent autonomous battlespace surveillance and reconnaissance. While this concept might seem far-fetched, it is supported by numerous technologies that are currently in use with underwater glider research. Some of these advancements include compact acoustic towed and tetrahedral arrays (Hughes et al. 2009, Maguer et al. 2013), onboard signal processing (Dassatti et al. 2011), and automated acoustic signal classification (Baumgartner et al. 2014).

This thesis evaluates underwater gliders as mobile, autonomous, passive acoustic sensing assets. Of specific interest are the ability of these platforms to loiter at depth and to exploit the reliable acoustic propagation paths present in a deep ocean environment. In this study an autonomous underwater glider functions as a node in a theoretical collaborative network with an unmanned surface vehicle (USV) that operates as a wireless acoustic communications relay, or gateway, node. Research demonstrates this is a functional network model with potential for future use (Bingham et al. 2012).

A thorough analysis of how to design and operate such a system is warranted. This study, however, considers two critical aspects of the inherent challenges: where to position the sensing platform in the water column and how to keep it there for an extended loiter. A field experiment and acoustic propagation modeling were performed to investigate these operational factors. Data analysis and results are provided to evaluate acoustic sensing performance during phases of a glider dive cycle and a deep loiter. Modeling of acoustic channel impulse response is included to support a theoretical analysis of acoustic communication performance for the proposed system.

THIS PAGE INTENTIONALLY LEFT BLANK

II. BACKGROUND

The U.S. Navy's Information Dominance Roadmap for 2013–2028 predicts innovative and covert solutions are needed to effectively counter modern adversaries that employ anti-access/area-denial (A2/AD) strategies (U.S. Navy 2013). One suggested solution is to develop autonomous vehicles that can gain access to denied environments and conduct environmental sensing. The report states that success in the "information-intensive combat environments of the future" will in part depend on the capacity of these vehicles to enhance battlespace awareness. The roadmap defines Battlespace Awareness (BA) as, "the ability to understand the disposition and intentions of potential adversaries as well as the characteristics and conditions of the operational environment." The report also identifies major elements of BA that the Navy needs to optimize in order to effectively meet future threats. Requirements for improved data collection and processing stand out from that list as elements of BA that will benefit from the contributions of unmanned systems. Autonomous vehicles that operate in the undersea domain are expected to play a vital role in this collaborative effort.

A. MOTIVATION FOR GLIDER USE

It is essential to select the ideal vehicle design to meet specific undersea mission requirements. The 2004 edition of the U.S. Navy's Unmanned Underwater Vehicle (UUV) Master Plan identifies vehicle classes that are deemed appropriate for a host of proposed missions. It recommends underwater gliders for the collection of environmental data in regions, "where battlespace dominance has not been achieved" (U.S. Navy 2004). Underwater gliders are a type of unmanned undersea vehicle (UUV) that use a buoyancy engine to move vertically and wings to move horizontally throughout the water column (Rudnick et al. 2004, Sherman et al. 2001). Underwater gliders use their sensors to characterize the oceanographic environment and, due to their unique method of operation, have far greater range and endurance than other unmanned undersea vehicles that utilize more conventional propulsion (Rogers et al. 2004). Proven designs, such as

the Slocum glider (see Figure 1) and the Spray glider (see Figure 2), are two-man portable as well as simple to deploy and recover.

Figure 1. The Slocum glider developed by Teledyne Webb Research as it is launched from a small boat.

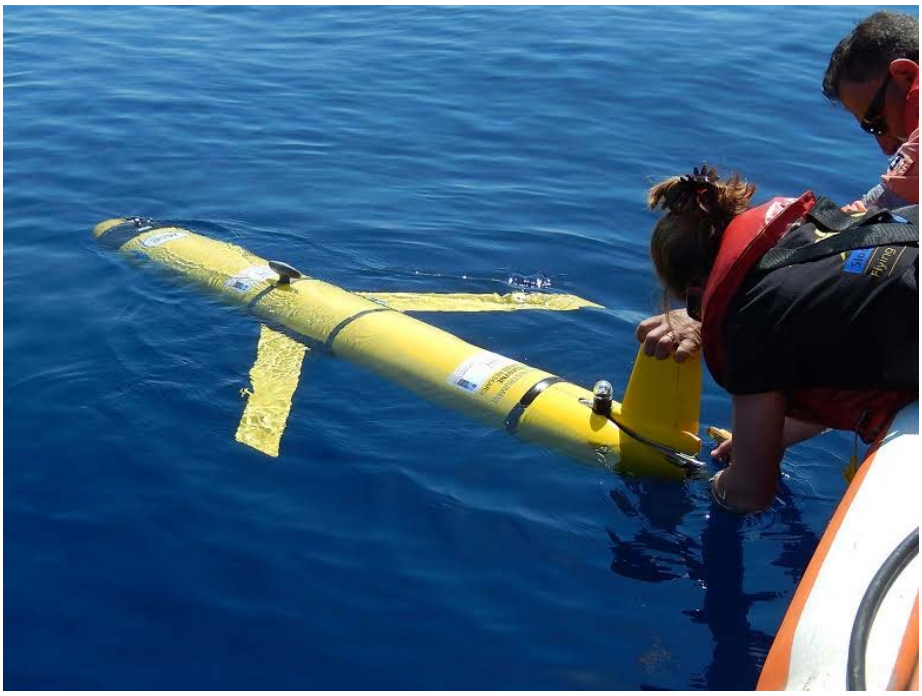

Slocum gliders have a modular payload design (Teledyne Webb Research 2015). Various models can operate at depths from 4–1,000 meters, for up to 365 days, with a max range of 6,000 km (from Naval Drones 2015, http://www.navaldrones.com/images/glider.jpg).

The UUV Master Plan also suggests that pre-positioned autonomous cueing assets will support future Anti-Submarine Warfare (ASW) and Intelligence, Surveillance, and Reconnaissance (ISR) missions (U.S. Navy 2004). The use of gliders for acoustic signal detection and classification is not specifically mentioned. However, in the decade since the publication of the 2004 UUV Master Plan these capabilities have been consistently demonstrated with various glider platforms. When outfitted with underwater acoustic receivers, known as hydrophones, and onboard signal processing capabilities gliders become quite effective mobile passive acoustic sensing platforms (Baumgartner et al. 2014). Regardless of the specific type of sensors, whether acoustic or non-acoustic, it is

quite easy to imagine how networks of such vehicles will help facilitate the transition from legacy methods of undersea environmental assessment.

Figure 2. The Spray glider.

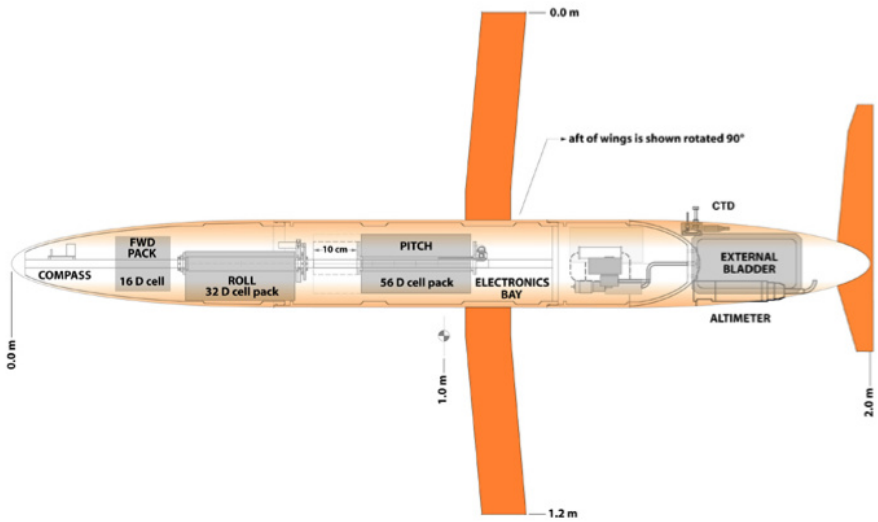

Cutaway diagram of the Spray glider developed by the Scripps Institution of Oceanography (SIO) and the Woods Hole Oceanographic Institution (WHOI). The battery packs, inside a sealed pressure hull, are mechanically shifted to control vehicle pitch and roll attitude. The external bladder, within the flooded science bay, fills with oil to change vehicle buoyancy. Antennas for satellite communications and GPS navigation, not depicted, are built into the glider's wings. Mission endurance can last six months and cover 3,600 km (from Scripps Institution of Oceanography 2015, http://spray.ucsd.edu/pub/rel/info/spray_description.php).

B. N2/N6 PROPOSED STUDY

Given the capabilities of currently available platforms, and the potential to execute missions with military relevance, a study of the integration of USVs and UUVs in support of wide-area environmental sensing and characterization has been proposed by the Deputy Chief of Naval Operations for Information Dominance (DCNO N2/N6). In support of this study a Naval Postgraduate School research proposal was submitted that outlines the concept of joining USV and UUV assets into a mobile, collaborative, and long-endurance network for both oceanographic and acoustic environmental characterization (Joseph and Horner 2014). The authors specifically hypothesize that, "the most critical component for effective UUV/USV integration is reliable cross-domain communications to effectively exchange navigation, command and control (C2) and

environmental information." This thesis expands on research questions presented in the proposal that encourage an evaluation of limitations that could impact the effective performance of such a system. The theoretical network framework described in the proposal is the foundation for the discussions presented in this study.

C. CONCEPT OF OPERATIONS

Conventional glider operations require routine trips to the surface to transmit recorded sensor data and vehicle status reports. Once on the surface, gliders establish a satellite communication link and report the requested data to distant controlling centers. Routine trips to the surface are also required for GPS signal reception in order to receive position updates and maintain accurate navigation. If a network of underwater gliders with passive acoustic sensing capabilities were to remain submerged, and thereby reduce the surface expressions of such a system, the vehicles would need a reliable and efficient method to transmit crucial data and receive position updates. This problem could potentially be solved through collaboration with a GPS-enabled USV and acoustic communications. This would allow an autonomous asset to persist at an ideal depth for its select suite of onboard sensors.

1. OPTIMAL SENSOR PLACEMENT

As acoustic energy propagates away from an underwater sound source it follows many paths that are individually influenced by physical parameters that change with range and depth. Variations in parameters such as temperature, salinity, and pressure affect how fast sound travels through seawater. As propagating sound waves encounter regions of the ocean with different sound speeds the waves respond by refracting. In the mid-latitudes and tropics the strength of this refraction is driven by the relatively rapid decrease in water temperature with depth. This occurs in a layer of the ocean known as the main thermocline that extends below the warmer surface layer. As ocean depth increases in this layer the rate of change for sound speed, known as the sound speed gradient, is negative and sound is refracted downward as it propagates away from a source. When a portion of the total radiated acoustic energy from a sound source follows

this downward refracting path to a receiver, without first interacting with the ocean surface or bottom, it is propagating along a Reliable Acoustic Path (RAP) (see Figure 3).

Figure 3. Reliable Acoustic Path.

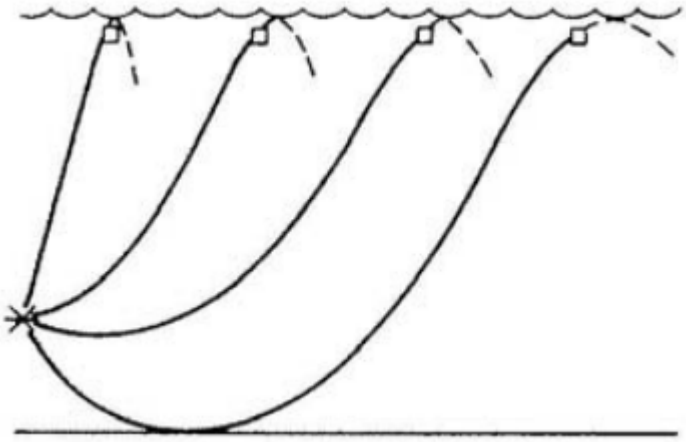

Depictions of various reliable acoustic paths that can exist between a deep acoustic source and a near-surface receiver (from Urick, R. J., 1983: *Principles of Underwater Sound:* Third Edition. Peninsula Publishing, 423 pp.)

The path is referred to as reliable because it is a direct path, from source to receiver, that avoids the boundary interactions that redirect and degrade acoustic signal intensity (Urick 1983). If a homogenous ocean is assumed then acoustic reciprocity implies this path can be exploited in reverse by simply alternating the locations of the source and receiver (Rayleigh 1894). This makes the RAP a valuable physical phenomenon of the deep ocean for both passive acoustic detection and acoustic communications. Given the low ambient noise levels at greater depths this enables a deep acoustic sensor to monitor a much larger area at a high signal to noise ratio (SNR) (Thompson 2009).

Because of these factors, there is great utility in having a sensing platform that can position itself at an ideal location in the water column, engage in a multi-month loiter, and sample the environment while it gets there. Optimizing sensor placement in this way increases acoustic detection ranges and time in contact. The field experiment

conducted for this study seeks to demonstrate these benefits by conducting environmental sampling in transit and during quiet loitering.

2. LONG-ENDURANCE LOITERING

Gliders and other undersea vehicles modified with underwater acoustic telemetry modems have demonstrated that trips to the surface to transmit data can at least be minimized when a USV (see Figure 4) acts as a network surface gateway platform (Maguer et al. 2013, McGillivary et al. 2012). Similar research has also shown that acoustic communications make it possible for a USV to send commands (Howe et al. 2010), as well as estimate the range and bearing to underwater gliders and thus serve as a navigation reference gateway (Bingham et al. 2012, Stanway et al. 2014).

Therefore, underwater acoustic communications provides one method to connect a distributed network of autonomous undersea and surface vehicles and enable long-endurance loitering. According to this system model, the portion of a glider's battery power normally allocated to operate a buoyancy engine would be available for tasks such as onboard signal processing and acoustic communications. This would be significant considering that it is not uncommon for conventional glider designs to allocate more than eighty percent of total battery power to buoyancy engine operation (Jenkins et al. 2003). A glider with passive acoustic sensing capabilities could then loiter at an optimal depth determined by its own environmental sensing, process data onboard, and quickly communicate critical information off-board without the need for trips to the surface. A distributed network of these platforms would then have a limited surface expression; one USV could coordinate with many gliders. Such a network has great potential to become a valuable asset for enhancing battlespace awareness.

While this method of collaboration can potentially reduce the long communication time-delays imposed by glider dive cycles, underwater acoustic communications is not a perfect solution. The underwater environment between any acoustic source and receiver, referred to as the acoustic channel, places limits on available transmission bandwidth. Transmitted signals must also contend with various physical challenges of the time varying undersea environment such as surface conditions,

bathymetry, and ambient noise levels (Rogers et al. 2004, Howe et al. 2010). As a result the rate that data successfully arrives at a receiver modem, known as network throughput, is much lower than more traditional methods for connecting communications networks. Therefore, acoustic communications must be utilized in an efficient manner in order to be a viable method of connecting such a network.

Figure 4. Autonomous Surface Vehicles (USVs).

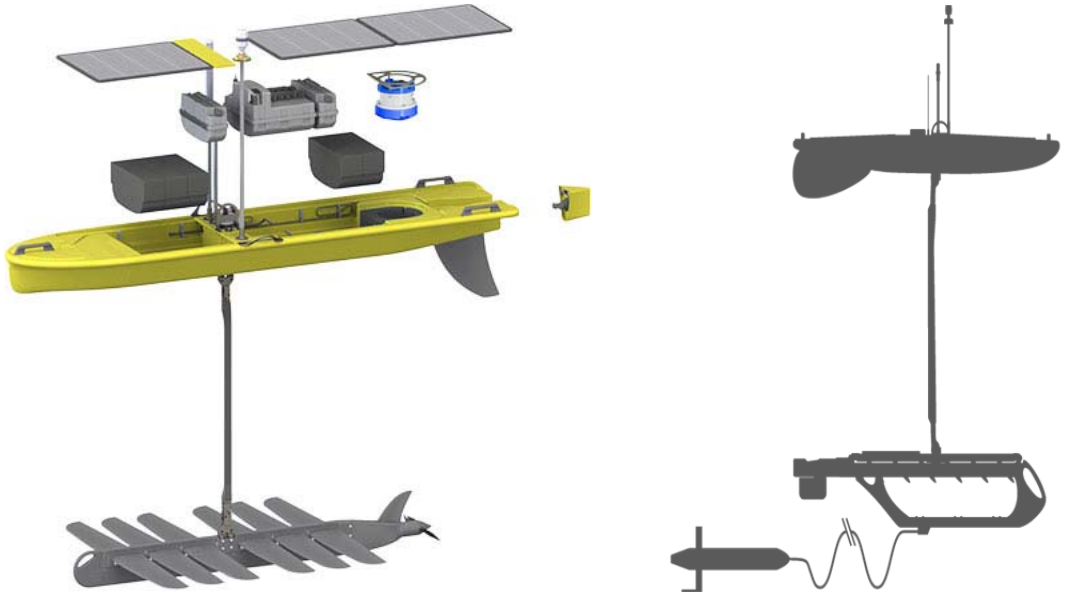

(a) (b)

Examples of autonomous unmanned surface vehicles (USVs) built by Liquid Robotics: (a) exploded view of the hybrid Wave Glider SV3 (from Liquid Robotics 2015, http://liquidr.com/technology/waveglider/sv3.html); (b) silhouette that depicts a Wave Glider SV2 modified to operate an acoustic modem housed in a towed body (from Liquid Robotics 2015, http://liquidr.com/resdown/resources/case-studies/cornell.html). The vehicles are solar-powered and utilize a customizable surface float to carry an assortment of computer payloads for environmental sensing, communication, and navigation. A tethered sub-surface platform with wings harnesses wave energy to propel the glider to waypoints.

THIS PAGE INTENTIONALLY LEFT BLANK

III. OCEAN ACOUSTICS

In order to understand why autonomous vehicles can use acoustics to passively sense the underwater environment and communicate with acoustic modems it is important to first understand how sound moves through water. Sound is a mechanical longitudinal wave of energy. A sound wave is set in motion in an elastic medium, such as seawater, by a vibrating source that creates pressure disturbances. In other words, sound travels through the ocean as pressure waves. Sound propagation in seawater can be described mathematically through solutions to the acoustic wave Equation (1) using appropriate descriptions of the boundaries and medium (Urick 1983).

$$\nabla^2 p = \frac{1}{c^2}\frac{\partial p}{\partial t^2} \tag{1}$$

The acoustic wave equation describes a three-dimensional change in acoustic pressure p with respect to position, time t, and sound speed c. Solutions to the equation explain how much of the original sound pressure remains after a signal travels a certain distance from a source. This technique enables computer models to numerically predict the motion and decay of acoustic wave energy in the ocean.

A common theoretical approach used to solve the acoustic wave equation in these models is known as ray theory. This geometric approach uses rays to trace the spatial path, or trajectory, of radiated acoustic pressure. The amplitude of acoustic pressure along the trajectory of a particular ray is then represented by the cross-section of a ray tube formed by adjacent rays. A detailed derivation of the ray theory approach and its application in computer-based models can be found in Jensen et al. (1994). A general overview of the theory and how it models sound propagation is provided below.

A. RAY THEORY

As previously described, the speed of sound in seawater plays a central role in determining how acoustic energy propagates. Sound speed in the ocean is a function of temperature, salinity, and pressure. Representations of its variation with respect to depth are called sound speed profiles. These variations in sound speed cause rays of acoustic

pressure energy to follow curved paths from source to receiver. This behavior is known as refraction and is described by an acoustic form of Snell's Law (Hovem 2013)

$$\xi = \frac{\cos\theta(z)}{c(z)} = \frac{\cos\theta_0}{c_0}. \tag{2}$$

While sound speed depends on depth $c(z)$, it has range-dependence as well. However, it is more straightforward to illustrate Snell's Law from a range independent perspective. If a medium is divided into horizontal layers with constant velocity the law explains that acoustic ray grazing angles at layer boundaries are directly influenced by the speed of sound in those layers (Urick 1983). As a result, incident rays change direction upon crossing a layer boundary. As these direction changes accumulate over distance and time, the ray path takes on the shape of an arc. This can be visualized by considering a particular segment of an arcing acoustic ray path (see Figure 5). The shape of the ray segment is defined by a change in range and depth, dr and dz, and its angle θ relative to the horizontal. When sound speed varies with depth, known as the sound speed gradient $g(z)$,

$$g(z) = \frac{dc(z)}{dz} \tag{3}$$

the ray angle θ will change according to Snell's Law. Ultimately, this means that the radius of curvature $R(z)$ for this ray path,

$$R(z) = \frac{c(z)}{\cos\theta(z)}\frac{1}{g(z)} = -\frac{1}{\xi g(z)}, \tag{4}$$

is also a function of depth (Hovem 2013). The ray parameter ξ defined in Equation (2) is a constant ratio. It is a unique value for a particular ray. The curvature of an acoustic ray is simply a function of this constant value and the sound speed gradient at a specific depth. The sign of the sound speed gradient indicates if the ray will curve upward or downward. This means that if sound speeds are trending slower with increasing depth, a negative gradient, acoustic rays will refract downward (see Figure 6). Ray tracing computer programs use these techniques to incrementally map out individual ray paths and calculate acoustic travel times to receiver locations.

Figure 5. Arcing acoustic ray path

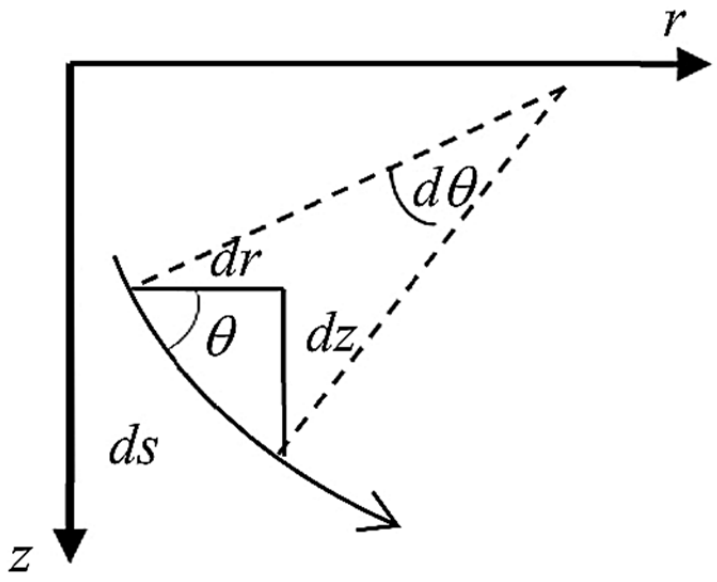

A ray path segment with an arc length ds in an isotropic medium (from Hovem, J. M., 2013: Ray trace modeling of underwater sound propagation. *Modeling and Measurement Methods for Acoustic Waves and for Acoustic Microdevices*, M. G. Beghi, Ed., InTech, DOI: 10.5772/55935).

Figure 6. Diagram of an acoustic ray trace

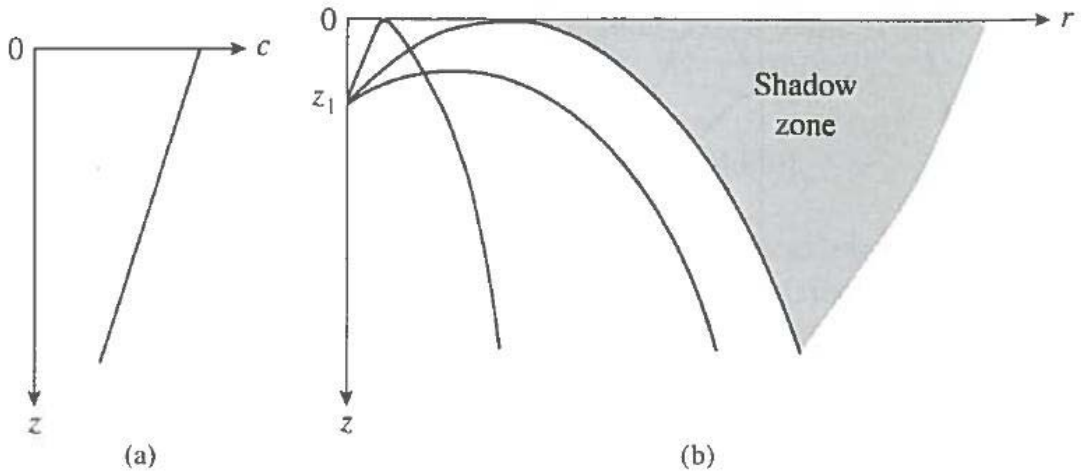

(a) a negative gradient sound speed profile; (b) representations of how acoustic rays with various initial angles will propagate from a source depth z_1 given the profile, as well the depiction of a "shadow zone" that forms at the limit of the tangential ray path (from Brekhovskikh, L. M., and Yu. P. Lysanov, 2003: *Fundamentals of Ocean Acoustics*. Springer, 280 pp.).

Once an ensemble of acoustic ray paths are calculated, ray tracing models must also calculate how acoustic pressures will change along the way. This is modeled by the varying cross section of a tube formed by adjacent acoustic rays (see Figure 7). This ray tube is considered to have constant acoustic power and its width dL is then proportional to the amplitude of acoustic energy at some distance from a sound source. The average acoustic pressure, or root mean square pressure p_{rms}, that moves through a unit cross-section of the tube for a unit time represents acoustic power flux and is called acoustic intensity I

$$I = \frac{p_{rms}^2}{\rho c}, \tag{5}$$

where ρ and c are seawater density and sound speed, respectively.

The "loudness" of sound at a location is simply a ratio of two intensities or pressures. When the ratio utilizes a standard reference intensity or reference pressure the result is a parameter known as sound pressure level SPL

$$SPL = 10\log\left(\frac{I}{I_{ref}}\right) = 10\log\left(\frac{p_{rms}^2}{p_{ref}^2}\right) = 20\log\left(\frac{p_{rms}}{p_{ref}}\right), \tag{6}$$

where $I_{ref} = 6.7\times10^{-19}\frac{W}{m^2}$, and $p_{ref} = 1\mu Pa$. This "loudness" is represented by the dimensionless logarithmic unit decibel (dB) and the associated reference parameter.

When sound pressure levels are calculated in the ray tube at one meter from a sound source, as well as at some distance r from the source, the comparison yields the estimated reduction in sound level due to propagation, or transmission loss TL

$$TL = 20\log\left(\frac{p(1m)}{p(r)}\right) = 10\log\left(\frac{I(1m)}{I(r)}\right) \tag{7}$$

However, this is only a geometric representation of how sound pressure changes as it propagates from a source. There are several other important factors to consider that influence transmission loss and they are commonly implemented in ray theory models. These will be discussed in the section that addresses the passive sonar equation.

Figure 7. Ray tube model

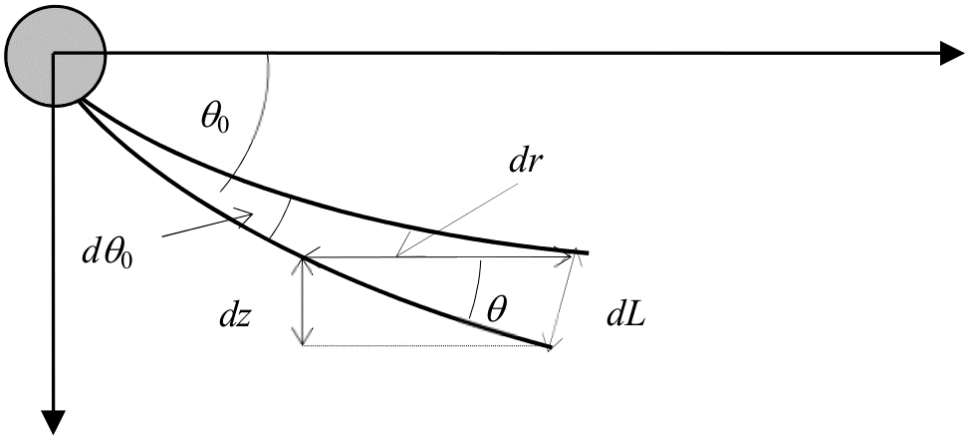

Acoustic intensity modeled with ray tubes. Range and depth increase along the horizontal axis and vertical axis, respectively. The gray circle represents a sound source with initial acoustic ray angle θ_0; $d\theta_0$ is the initial separation between two rays; dr is an increment in range; dz is the depth difference between the two rays; and dL is the ray tube width (from Hovem, J. M., 2013: Ray trace modeling of underwater sound propagation. *Modeling and Measurement Methods for Acoustic Waves and for Acoustic Microdevices*, M. G. Beghi, Ed., InTech, DOI: 10.5772/55935).

B. MODIFIED RAY TRACING

While the traditional ray tracing method is computationally fast, it has several important limitations. It produces excellent results for higher acoustic frequencies (e.g., > 1 kHz), but fails at lower frequencies. This is due to the fact that ray tracing produces approximate solutions to the wave equation. It does this through an assumption that the scale of the sound speed gradient is much larger than the acoustic wavelengths. This is fine for higher frequencies where wavelengths are short. Lower frequencies, however, with longer wavelengths make this critical assumption inappropriate (Urick 1983). Other models based on normal mode theory and the parabolic equation method produce exact solutions for a wider range of frequencies but can be computationally expensive. Approximations produced by ray tracing also incorrectly predict infinite acoustic intensity or no acoustic intensity at regions known as caustics and shadow zones, respectively. However, a modified ray tracing model known as Bellhop overcomes these limitations and produces predictions in excellent agreement with exact solution models (Porter 2011). This model was chosen for use in this study, but it is important to note that

it is not a complete replacement for exact solution methods. Its strengths and limitations are explained in the next chapter.

C. THE PASSIVE SONAR EQUATION

Acoustic sensing and acoustic communications are fundamentally similar in that both rely on the successful detection of sound at some distance from a source. Ray theory shows that acoustic signal energy will dissipate as it propagates along various underwater paths. Acoustic receivers must then detect the presence of this signal amid the background noise. Detection is therefore an analysis of the input signal-to-noise ratio to uncover signals that sufficiently exceed the noise level (Urick 1983). This process requires an application of a threshold that once exceeded results in a conclusion that the signal of interest is present in the noise. The threshold must strike an important balance between two competing factors: probability of detection and probability of false alarm. This is a challenge because when the threshold is too high both the probability of detection and the probability of false alarm are low. When set too low, both probabilities are high (Urick 1983).

The proper balance depends on the environment, sonar system design, and signals of interest. Signals and noise, however, are affected by the environmental variability in the ocean that induces acoustic uncertainty. As a result, these vital parameters constantly fluctuate from one instant to the next. Each parameter is a stochastic, or random, process that can only be estimated.

In order to predict the performance of an acoustic detection system it is necessary to establish a relationship between the passive sonar parameters: source level (SL), transmission loss (TL), noise level (NL), directivity index (DI), and detection threshold (DT). This working relationship is known as the passive sonar equation (Urick 1983).

$$SL - TL = NL - DI + DT \tag{8}$$

It is important to keep in mind that this simple equation represents a relationship among parameters with inherent uncertainty and does not reduce underwater acoustics to simple deterministic solutions. The directivity index (DI) describes the ability of the receiver to resolve acoustic detections from a particular bearing. In the case of this study,

an omnidirectional receiver is used so DI can be set to zero. The detection threshold (DT) represents the minimum remaining signal at a receiver, in excess of the noise level (NL), that is required for a detection. This implies that the passive sonar equation can be written in terms of a signal-to-noise ratio (SNR).

$$SL - TL - NL = SNR \tag{9}$$

With this arrangement detections are theoretically possible as long as the signal-to-noise ratio is greater than zero (e.g., signal can break out of the noise).

The source level (SL) is simply the sound pressure level radiated at one meter from the acoustic source, and the transmission loss (TL) is the reduction of that sound level due to propagation losses. As mentioned previously, the ray tube model describes transmission loss according to geometric spreading of the acoustic energy, but it is not the only important physical process involved.

In addition to the geometric spreading of a sound signal, transmission loss also includes losses due to absorption, scattering, and diffraction. Collectively, these represent loss due to attenuation (Urick 1983). Absorption, also known as volume attenuation, is the conversion of acoustic energy into heat energy that is transferred to the seawater. It involves a frequency-dependent response to fluid viscosity, as well as magnesium sulfate and boric acid molecules found in seawater (Francois and Garrison 1982). As a result, its influence on transmission loss cannot be mitigated. If desired, however, the Bellhop model can factor in the impact of seawater absorption when performing transmission loss calculations.

Losses due to scattering from a rough sea surface and diffraction are minimized when a receiver is within range to detect signals along a direct path or reliable acoustic path (RAP) and will not be covered in this discussion. However, surface reflections and scattering are an important concern when attempting to optimize acoustic modem performance in shallow water environments.

Finally, if any excess acoustic energy remains after the impact of transmission loss an acoustic receiver still must contend with the noise level to make detections. Noise is the combination of background, or ambient, environmental noise and receiver self-

noise. Underwater ambient noise is commonly generated by surface winds, precipitation, shipping vessel density, biologics, and seismic activity (Urick 1983). It can be filtered out at a receiver if it does not impact the portion of the frequency spectrum that contains the signal of interest. Self-noise, however, can be a greater challenge especially for underwater gliders that were not originally designed as passive acoustic platforms. Nevertheless, the predominantly silent operation and mobility of gliders make the vehicles very appealing for acoustic sensing research.

IV. ACOUSTIC SENSING EXPERIMENT

An experiment was conducted in February 2015 on the north side of Monterey Canyon at Smooth Ridge to assess the acoustic recording performance of an Unmanned Underwater Vehicle (UUV) as it transitioned into a deep loiter. A medium frequency underwater acoustic transducer provided the source signals and a Spray glider, equipped with an acoustic recorder, served as the mobile sensing platform. Previous research (Baumgartner et al. 2014) demonstrates that autonomous underwater gliders can detect and classify underwater marine mammal calls when given the capability to process acoustic signals onboard. The goal in this experiment was to intentionally broadcast continuous wave (CW) signals and evaluate their reception throughout the descent, deep loiter, and ascent dive cycle phases of an autonomous underwater glider. Experiment geometry was planned to demonstrate that a mobile glider can relocate from the acoustic shadow zone in order to exploit reliable acoustic propagation paths. To simplify the design requirements for this demonstration, onboard processing capabilities were not implemented. All recorded data was processed following the recovery of the glider.

A. THE BELLHOP ACOUSTIC PROPAGATION MODEL

The Bellhop model was used during this study to produce acoustic propagation predictions that supported planning the experiment geometry, comparing observed transmission loss with calculated theoretical levels, and assessing acoustic communications performance. The model is designed to address the previously described fundamental physics problems of underwater acoustics, namely, what path will sound take underwater and what will happen to the original acoustic energy along the way.

Formally, Bellhop is a Gaussian beam tracing model that was developed to solve acoustic wave propagation problems and predict acoustic pressure fields in the ocean (Porter and Bucker 1987). For a given frequency, it uses a fan of beams to approximate an acoustic source and traces those beams as they propagate throughout a simulated underwater environment. The beams themselves are the model for how the original energy, or acoustic pressure, decays as it propagates through the ocean. This is

accomplished by associating each acoustic ray path with a beam model and a corresponding energy profile that decays according to a Gaussian distribution (Porter and Bucker 1987). This approach enables the calculation of acoustic pressure values for a range of receiver locations by "summing the contributions of each of the individual beams" (Porter and Bucker 1987). These design features allow the Bellhop model to produce better predictions than basic ray tracing methods and still be computationally efficient (Porter 2011).

1. Model Inputs

Input data is provided to the model in an environmental file (see Appendix A) that contains, at minimum, a sound speed profile and descriptions of the ocean surface and bottom boundaries. This file also allows a user to set the acoustic source frequency, enable the calculation of frequency-dependent volume attenuation, and define source and receiver geometry. When deemed necessary the model has the additional options to implement range-dependent sound speed and bottom profiles, as well as define ocean surface roughness.

a. Sound Speed Profile

The Spray glider used in this experiment is equipped with a pumped conductivity, temperature and depth (CTD) sensor that records fine resolution data during the ascent portion of its dives. After the completion of a dive, these observations were used to create the sound speed profile (SSP) for use in the Bellhop model environmental input file. This was accomplished through the use of a MATLAB script (Morgan and Pender 2003) that converts the temperature, salinity, and pressure measurements to sound speeds using the UNESCO "Sound Speed in Seawater" polynomial (Fofonoff and Millard 1983).

An initial SSP was created with data from a dive conducted the day prior to the experiment. It was used to generate the acoustic transmission loss predictions necessary for selecting an ideal source-to-receiver range to meet our objectives. Subsequent Bellhop model runs were conducted using the SSP created from data collected during the experiment dive. This was done to simulate an acoustic propagation model that could theoretically run aboard an autonomous vehicle and perform calculations with real-time

oceanographic data. All model runs were conducted with range-independent sound speed profiles. This approach uses a single sound speed profile to model the ocean between an acoustic source and receiver. While inappropriate for long range problems, this was considered an acceptable approximation given the small scale of the experiment (< 6 km propagation paths) and the relatively level ocean bottom.

Figure 8. Bellhop input Sound Speed Profile (SSP)

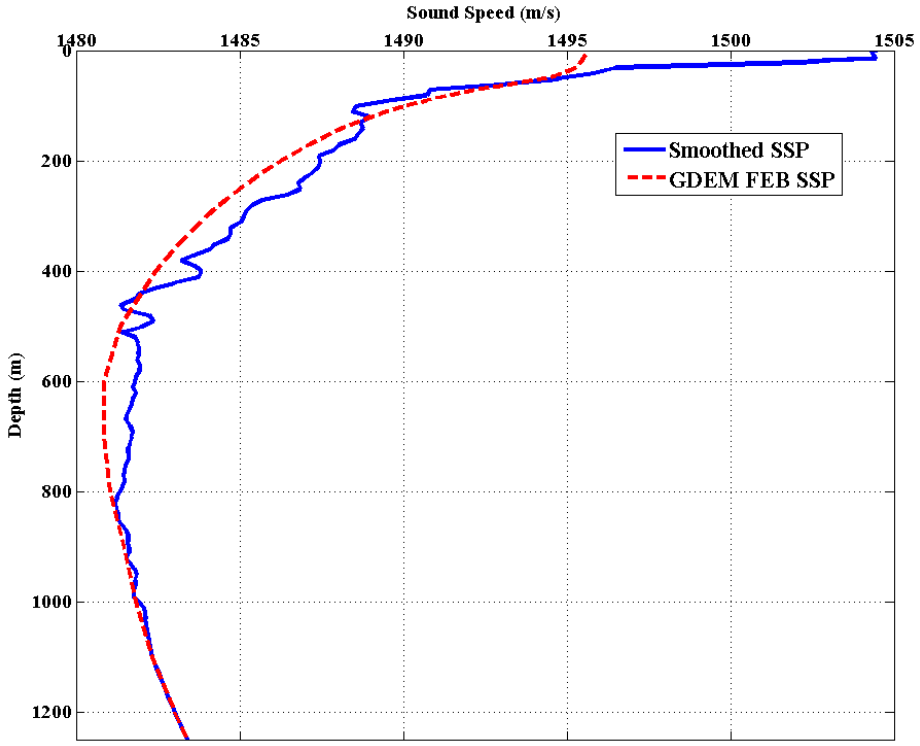

The solid line indicates the SSP derived from Spray glider observations the day prior to the experiment after the resolution was smoothed to 10 m using linear interpolation. The dashed line is a February SSP from the GDEM database that was used to extend the glider profile to the local bottom depth.

Testing revealed that a 10 m sub-sampled version of this SSP using linear interpolation provided adequate model resolution and eliminated undesirable and improbable artifacts in the model predictions (e.g., multiple fine scale ducts and channels). Smoothing of a SSP in this way is recommended in the Bellhop literature as a means to mitigate the influence of small localized SSP features on output predictions as

well as manage model run time (Porter 2011). Additionally, glider dives achieved maximum depths short of the bottom so the sound speed profiles were extended with climatological data from the U.S. Navy Generalized Digital Environmental Model (GDEM) database maintained by the Naval Oceanographic Office.

b. Ocean Surface and Bottom Boundaries

Acoustic energy interactions with the ocean surface and bottom induce signal direction changes according to the reflectivity of the boundaries. Given a particular source-to-receiver geometry and environmental conditions these boundary interactions can result in a complicated arrival structure. These multipath arrivals (see Figure 9) create interference effects at a receiver such as amplitude fading and signal distortion that can present challenges for both passive signal detection and acoustic communications. The Bellhop model can more accurately predict the presence and parameters of multipath arrivals when provided with realistic or range-dependent bathymetry data and ocean surface shape estimations.

To tailor the model predictions in this study to the local environment the initial and terminal Spray glider dive coordinates were used to extract along-track bathymetry from a U.S. Geological Survey (USGS) database (Maher et. al 2001). This information was then used in a range-dependent Bellhop bathymetry file to define the ocean bottom. While surface-reflected and bottom-reflected acoustic rays were no doubt present during the in-field test, experiment geometry was specifically chosen to demonstrate the transition between the shadow zone and the lower loss downward refracting direct path rays. Nevertheless, estimates of ocean bottom geo-acoustic parameters were incorporated into the Bellhop environmental input file for completeness (see Appendix A). The option to alter the ocean surface shape in order to approximate surface roughness, or variability, was not utilized in the modeling runs. Instead, the default flat representation of the ocean surface was used. However, a small degree of transmission loss from surface interaction was expected due to the forecast light wind conditions.

2. Assumptions and Limitations

While the ray tracing capability of Bellhop greatly assisted with planning the experiment, it is necessary to address two model limitations and assumptions that were made. First it is important to emphasize that the output of a Bellhop model run is a collection, or ensemble, of deterministic calculations. This means that given the set of user-specified inputs, the model will produce the same output every time. However, the unique ensemble of deterministic calculations does not represent a deterministic forecast. Instead, it is an estimation of the likely behavior of acoustic energy given the user-provided initial conditions (Porter 2011). This is because the initial conditions are themselves a snapshot representation of small scale ocean features that randomly change over time.

In other words, because of environmental uncertainty it is difficult to achieve truly accurate predictions from a single run of a model such as Bellhop. To incorporate random variation, such as surface roughness, the model would need to be run many times with variable input data. A probabilistic, or stochastic, forecast could then be generated from a statistical analysis of the resulting ensemble of model runs. While the development of efficient statistical acoustic channel simulators is common, particularly in acoustic modems research (Llor and Malubres 2013, Dol et al. 2013), we will assume that individual Bellhop predictions are sufficient for our purposes in this study.

Secondly, a Bellhop prediction is a two-dimensional representation of the water column between source and receiver. It does not account for shifting bearings between a source and receiver over a period of time. However, given the anticipated source-to-receiver range, experiment duration, and average glider velocity, separate predictions for individual bearing lines are not deemed necessary. We therefore assume that a single Bellhop model run is sufficiently accurate to estimate ray paths and transmission loss along all of the changing bearing lines between the source and receiver.

B. EXPERIMENT GEOMETRY

Acoustic transmission loss predictions were examined to identify an ideal glider range and depth pair, relative to the sound source, that would promote exposure to the

downward refracting sound (see Figure 9). Based on the planned loiter depth of 1000 m a source-to-receiver range of 5.5 km was selected. The ship with the sound source was then positioned relative to the glider dive cycle to achieve our objectives: observe the increase in signal intensity as the glider transitioned from the shadow zone to the region dominated by reliable acoustic propagation paths. A broadside aspect, with respect to the glider dive cycle, was chosen for acoustic signal transmissions (see Figure 10). This was done to simplify range estimation and facilitate a comparison between observed and predicted transmission loss as a function of depth. The broadside aspect also ensured the glider would be in position to take advantage of reliable acoustic paths during its deep loitering.

Figure 9. Bellhop acoustic transmission loss prediction

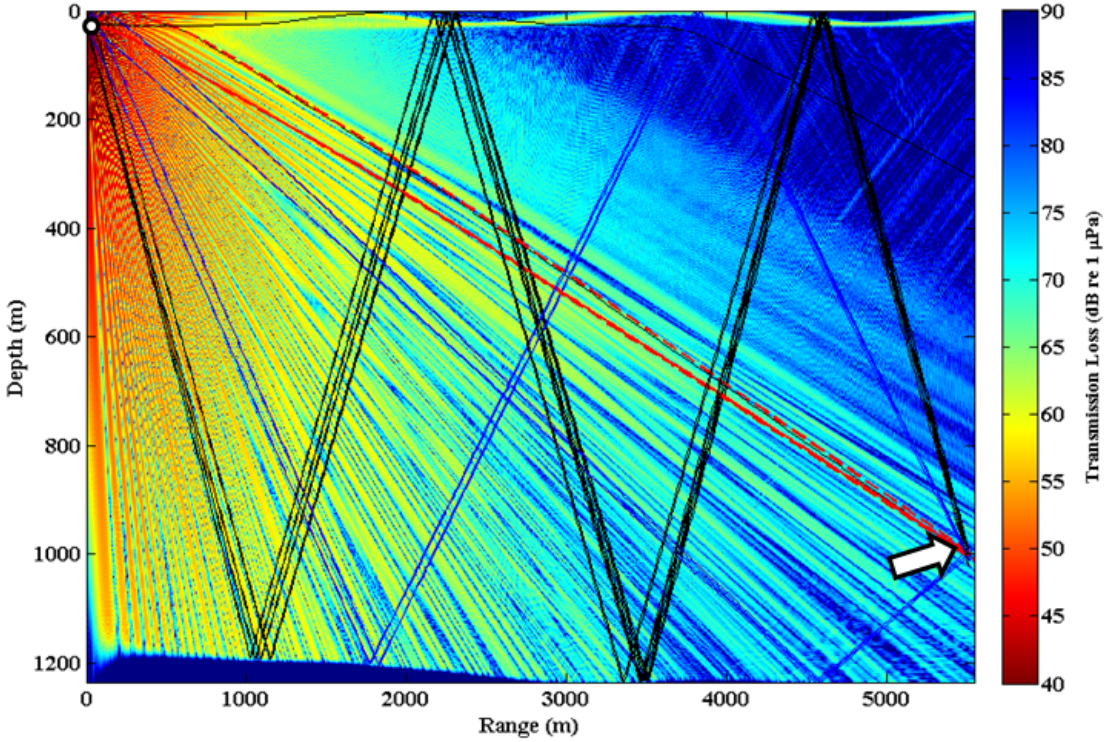

Acoustic transmission loss (TL) output prediction for a 2 kHz sound source (circle) at a 25 m depth with an eigenray plot overlay. An eigenray plot depicts the multiple ray paths that will arrive at a receiver given its specified range and depth from a sound source. The rays intersect (arrow) at the chosen glider depth of 1000 m and 5.5 km range from the sound source. The dashed lines depict the reliable acoustic path rays that have not interacted with the bottom boundary. Note the surface duct predicted as a result of the small scale features that the SSP in figure 8 describes at shallow depths.

Figure 10. Acoustic sensing experiment geometry

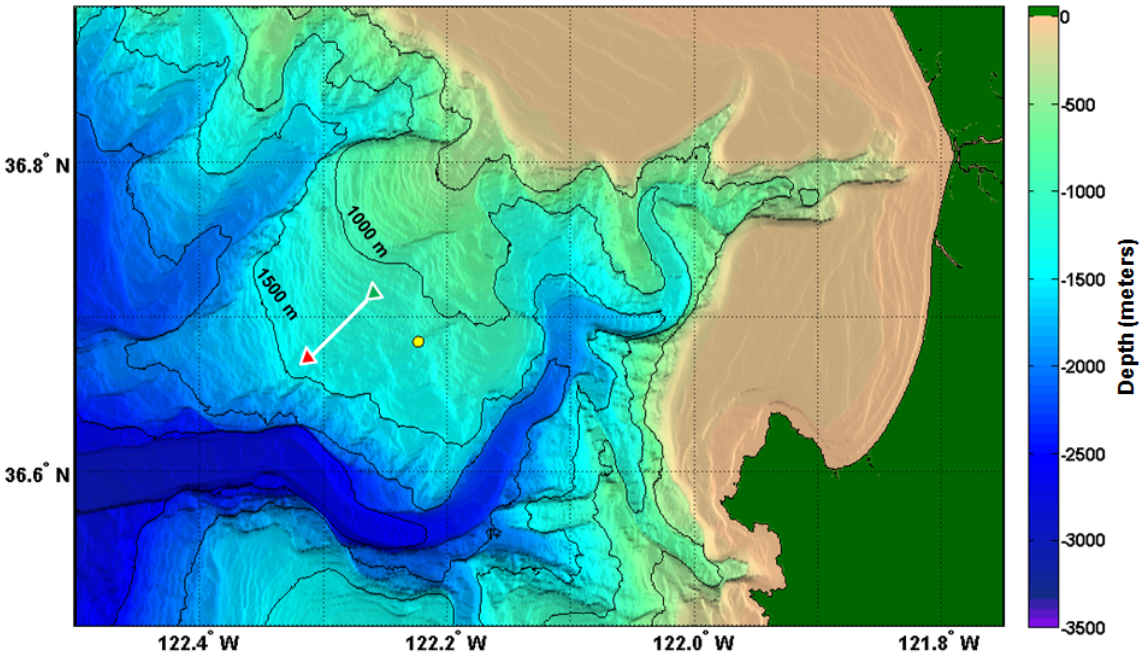

An overhead view of the location and associated bathymetry selected for the passive acoustic sensing experiment conducted on 24 February 2015. The experiment geometry, relative to Monterey Bay, is represented by the surface track approximation of the glider dive from start (green arrow) to finish (red arrow), and the relative location of the sound source (yellow circle).

C. DATA COLLECTION

Two Acousonde 3A recorders (see Figure 11) were used in this experiment; one monitored the medium frequency acoustic source levels, and the other served as the acoustic receiver aboard the Spray glider. The Acousonde is a miniature, self-contained, autonomous underwater acoustic recorder (Acoustimetrics 2015). The recorders were programmed prior to the experiment (see Appendix B), and the unit aboard the Spray glider utilized an external battery pack to achieve nearly a month of continuous acoustic recording prior to the test day.

Figure 11. Acousonde 3A underwater acoustic recorder

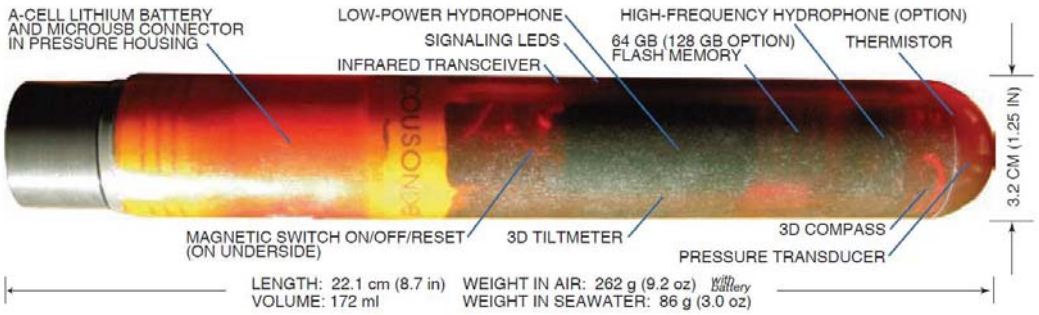

From Acoustimetrics 2015, http://www.acousonde.com/downloads/Acousonde3A_Brochure.pdf.

1. Source

Acoustic signals were broadcast using a U.S. Navy Type G34 mid-frequency transducer (see Figure 12) provided by the Underwater Sound Reference Division (USRD) of the Naval Undersea Warfare Center (NUWC). It was deployed via winch cable from the stern of the R/V *Fulmar* and powered by a shipboard amplifier. A MATLAB routine was used to sequence the broadcast commands to a signal generator, and a handheld GPS unit was placed at the stern of the vessel to establish a record of signal transmission locations. Source levels were monitored by an Acousonde attached to the winch cable. A source depth of 25 meters was chosen to simulate a shallow contact. The depth also serves as a reasonable proxy for an acoustic modem housed in Wave Glider underwater towed body. Broadcast frequencies of 2 kHz and 4 kHz were selected for their stable narrowband reproduction by the G34 transducer. Unfortunately, difficulties with the power amplifier and G34 wet mate connectors reduced the time and output voltage available for signal transmissions. Despite these constraints, acoustic signals were successfully broadcast during crucial portions of the deep glider dive and loiter.

Figure 12. Type G34 transducer ready to deploy from R/V *Fulmar*

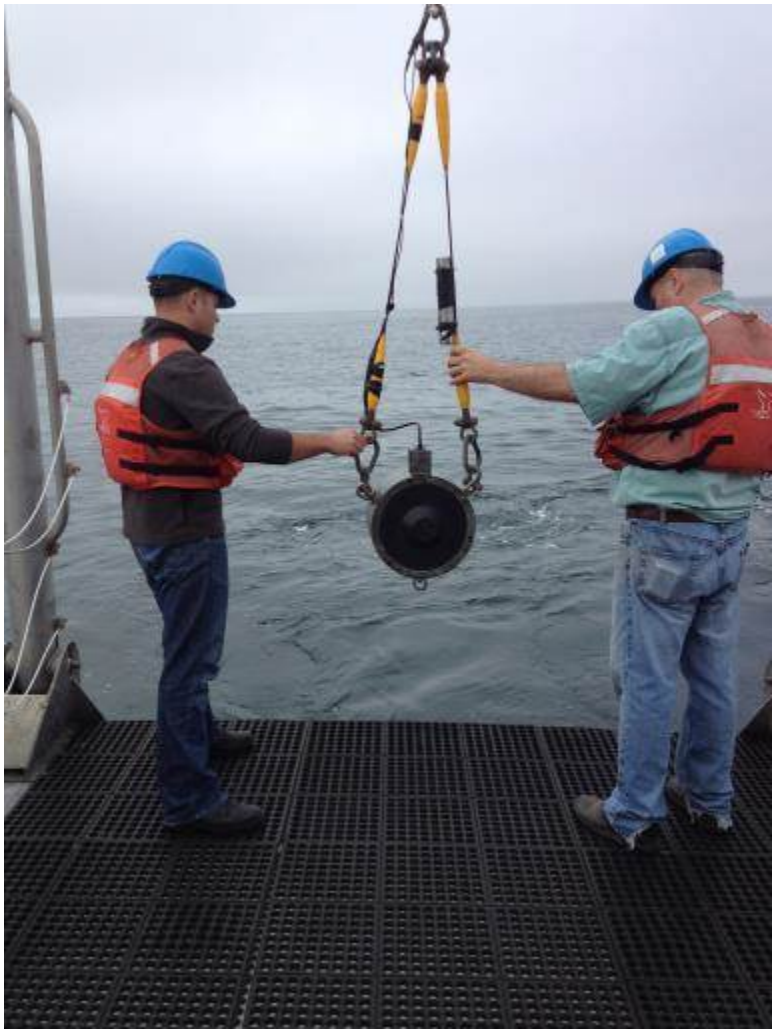

2. Receiver

The second Acousonde recorder was mounted inside the Spray glider science bay and received the signals from the G34. This specific mounting location was chosen because it is an extremely simple and fast method to provide an acoustic recording capability to a Spray glider without vehicle modification. Admittedly, this places the recorder in close proximity to sources of glider self-noise such as the pumped CTD and buoyancy engine electric pump motor. It also degrades the omnidirectional recording capability of the Acousonde because the science bay components, and potentially the pressure hull itself, can acoustically mask the hydrophone. Therefore, this is not

recommended as a permanent location for a hydrophone on the Spray glider platform. Unfortunately, unexpected R/V Fulmar repairs delayed the execution of the experiment. As a result, upon recovery it was discovered that the Spray glider Acousonde had reached its storage limit prior to the glider's ascent back to the surface (see Figure 13).

D. DATA PROCESSING

An initial review of glider data revealed that the dive cycle was completed in 6 hours and 26 minutes. It included 57 minutes of loitering at a depth of approximately 1000 meters, and covered a surface distance of 5.8 kilometers.

Figure 13. Spray glider acoustic experiment dive

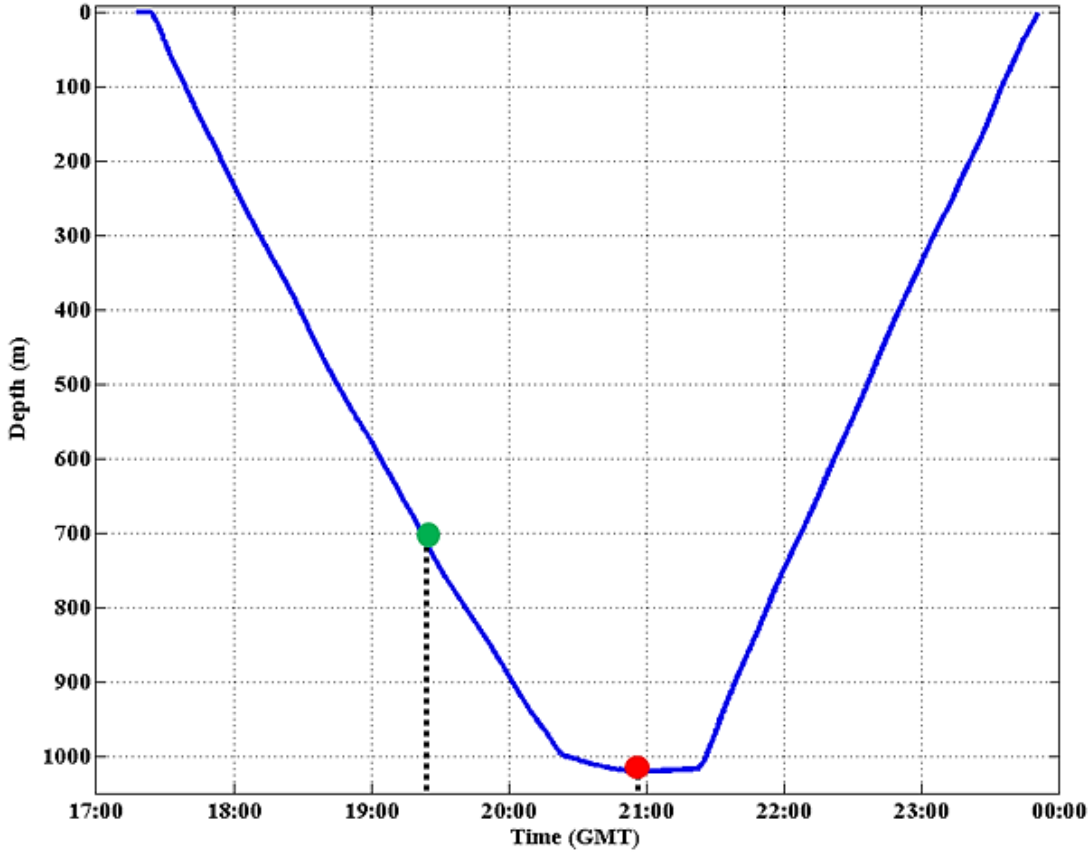

The dashed line and circle (green) indicate when signal transmissions began after troubleshooting delays. The second circle (red) marks the time when the Acousonde aboard the Spray glider reached its internal storage capacity.

Once the glider was recovered, the data from both Acousonde recorders was downloaded and portions applicable to the signal broadcast times were read into MATLAB. The companion MATLAB script (acousonderead.m) automatically accounts for receiver sensitivity and amplifier gain. The script reads the recorded data, for an indicated period of time, and calculates acoustic pressure values in micropascals (μPa) (Miller 2013). Once in this format, the acoustic signal data can be transformed from the time domain to the frequency domain using spectral analysis. This digital signal processing technique uses the Fast-Fourier Transform (FFT) to estimate the average acoustic power of digitally-sampled data with respect to its frequency spectrum (Johnson 1989). The relationship between acoustic power and frequency is known as power spectral density (*PSD*) and is often represented in decibels (*dB*) per hertz (*Hz*) (Stoica and Moses 2005). When acoustic pressure data for a particular time interval is transformed in this fashion the resulting *PSD* time series plot format is commonly referred to as a spectrogram. For large data sets, a technique known as the Long-Term Spectral Average (LTSA) can be used to present the output of spectrogram calculations in a compressed format for quick identification of signals (Scripps 2015).

With these techniques, source level estimates for the transmission frequencies were easily extracted from the G34 Acousonde power spectrum time series (see Figure 14 and Figure 15). A transmission loss correction was then applied to these values because the Acousonde reference distance was greater than one meter from the center of the G34 transducer. The result is a source level time series that can be used to calculate observed transmission loss when compared to data recorded on the Spray glider.

Figure 14. Spectral analysis of source level data

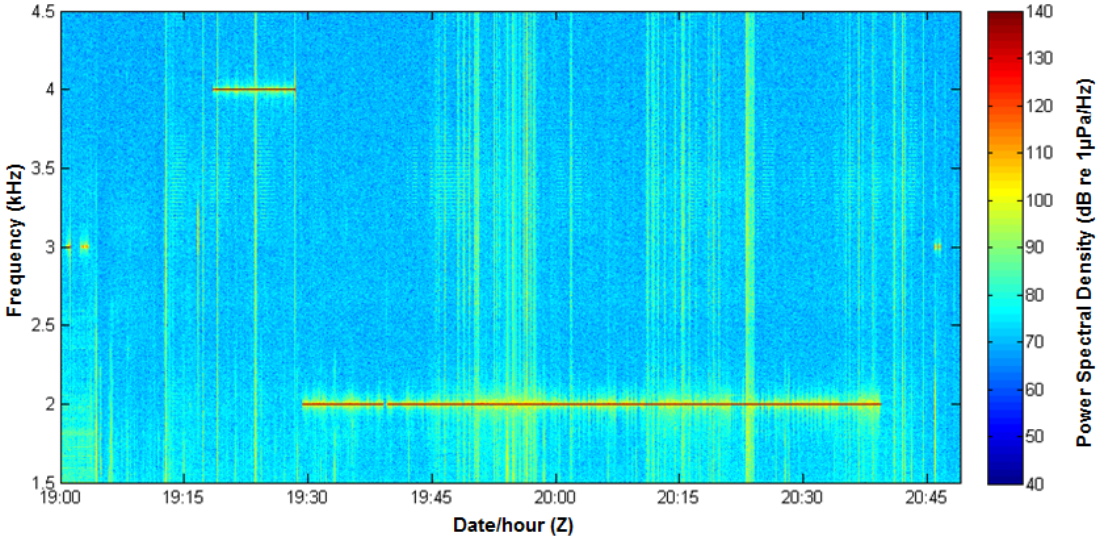

A Long-Term Spectral Average (LTSA) time series (3 second averaging window, 1 Hz bins, 29 kHz sampling frequency) produced from the G34 source level reference Acousonde. Broadcast intensity and duration of the 4 kHz and 2 kHz signals is clearly visible above ambient noise spectrum level (SNR > 0).

Figure 15. G34 4 kHz signal source level

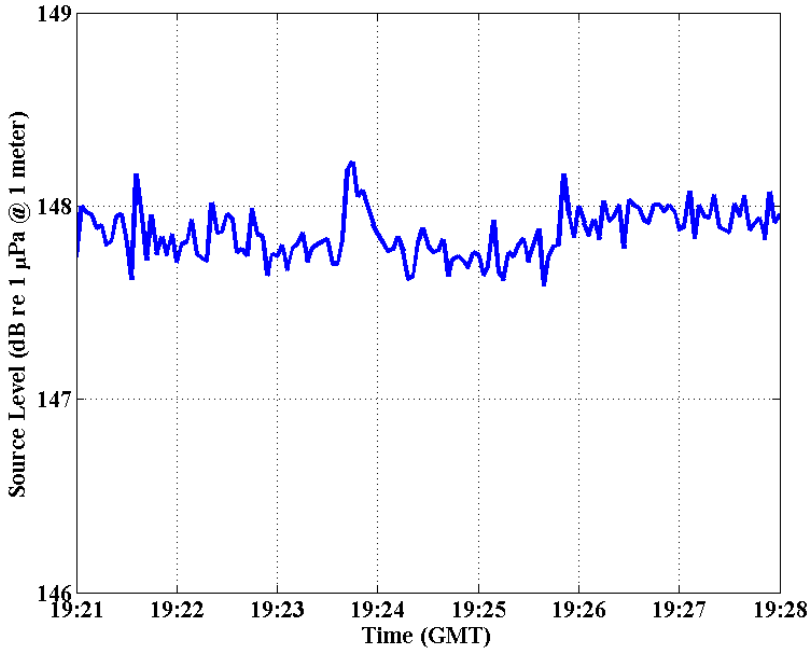

A sample of the 4 kHz signal source level derived from the data depicted in figure 14. A transmission loss correction, assuming spherical spreading loss, has been applied to adjust Acousonde pressure data for the 1.7 meter reference distance from the G34. Note the stability of the source signal amplitude with a variation of much less than 1 decibel.

The acoustic data set from the Spray glider proved to be useful in several ways: it contains over three weeks of acoustic ambient noise and marine mammal recordings, as well as an hour and a half of received signal data from the descent and loiter phases of the glider experiment dive. Compared to the G34, calculating acoustic receive levels at the Spray glider proved to be a more involved process due to unanticipated sources of noise.

1. Ambient Noise Filtering

In order to verify that the Bellhop model provided good predictions for setting up the experiment geometry, it was necessary to compare the transmitted signal intensity to the intensity recorded at the receiver aboard the Spray glider. Under typical conditions we could simply show that the signal energy level at the receiver, for the corresponding broadcast frequencies, was consistently observed above the ambient noise level. Unfortunately, the unanticipated and powerful acoustic air gun blasts of a nearby geological survey vessel made this a more challenging task (see Figure 16).

Figure 16. Geological survey noise spectrogram

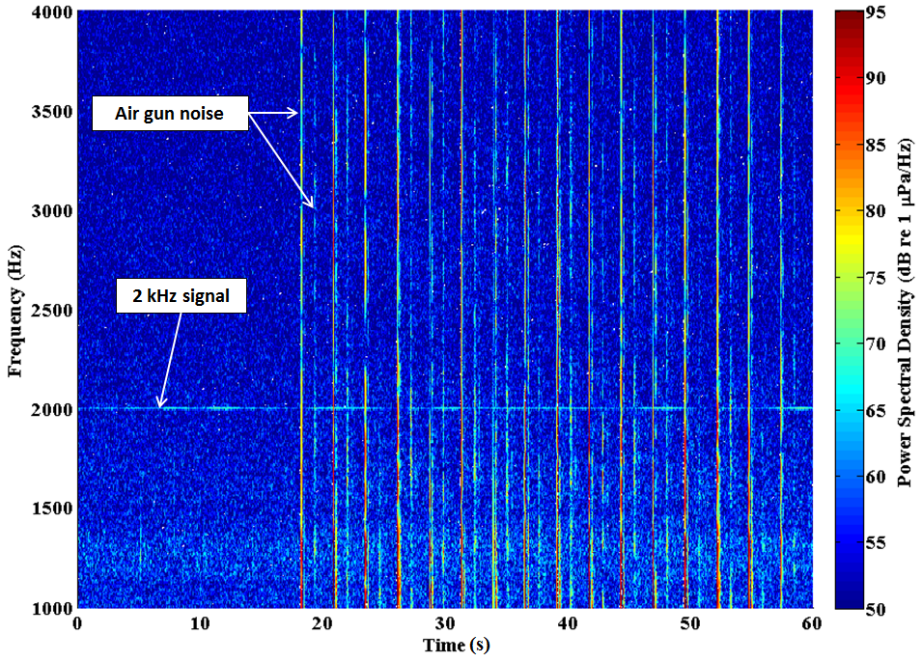

In this sample of data from the Spray glider the acoustic air gun blasts begin around the 18 second mark and contaminate the receive level estimates in the acoustic source frequency band (2 kHz).

When fired, the broadband acoustic intensity of these air gun blasts often surpassed the received narrowband intensity of the signals sent by the G34. Therefore, it was necessary to filter out these unwanted energy spikes from the received data. A MATLAB script was devised to read-in data and identify times when acoustic pressures exceeded a threshold that corresponded to air gun blasts and echoes. The stored times, along with a window matched to the average noise duration, were then used to ignore pressure data that would have otherwise introduced an unwanted bias in transmission loss assessments (see Figure 17). This technique revealed that 9% of the 10-minute 4 kHz data set, and 20% of the 80-minute 2 kHz data set, was masked by the air gun noise.

Figure 17. Air gun noise filtering example

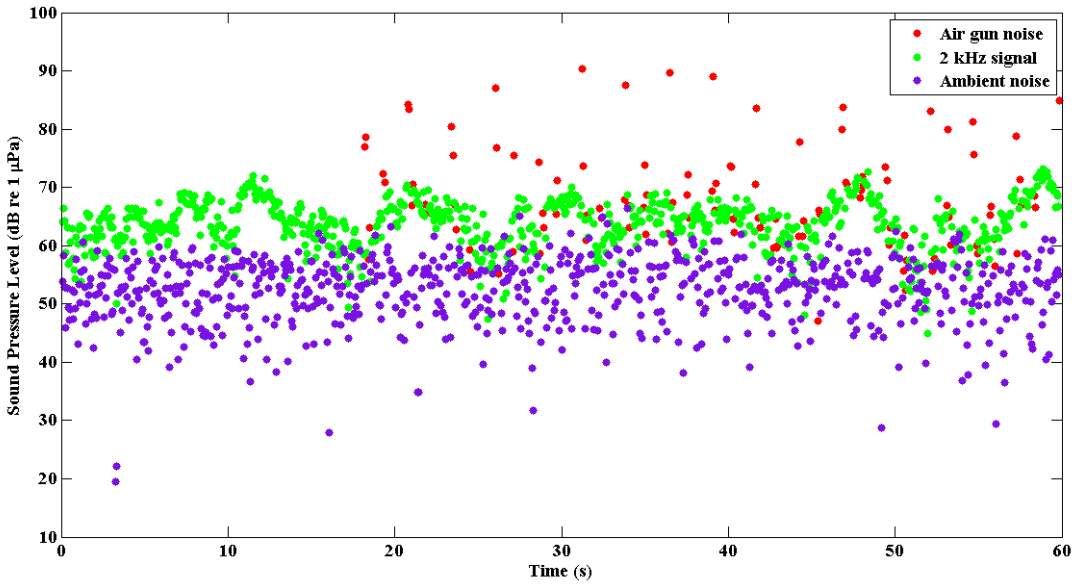

Signal data (2 kHz band) from the same time period as the spectrum displayed in figure 16 after data points that correspond to air gun impulse and echo noise have been identified for exclusion (red). Ambient noise is plotted as a visual representation of the signal-to-noise ratio (SNR) present at the receiver.

Once air gun noise is identified and excluded from the data, the remaining ambient noise levels are quite comparable to the empirically derived predictions (Wenz 1962) for the source frequencies, 4 kHz and 2 kHz, given the prevailing environmental conditions (e.g., Sea State 1).

Figure 18. Wenz curves for ocean noise levels

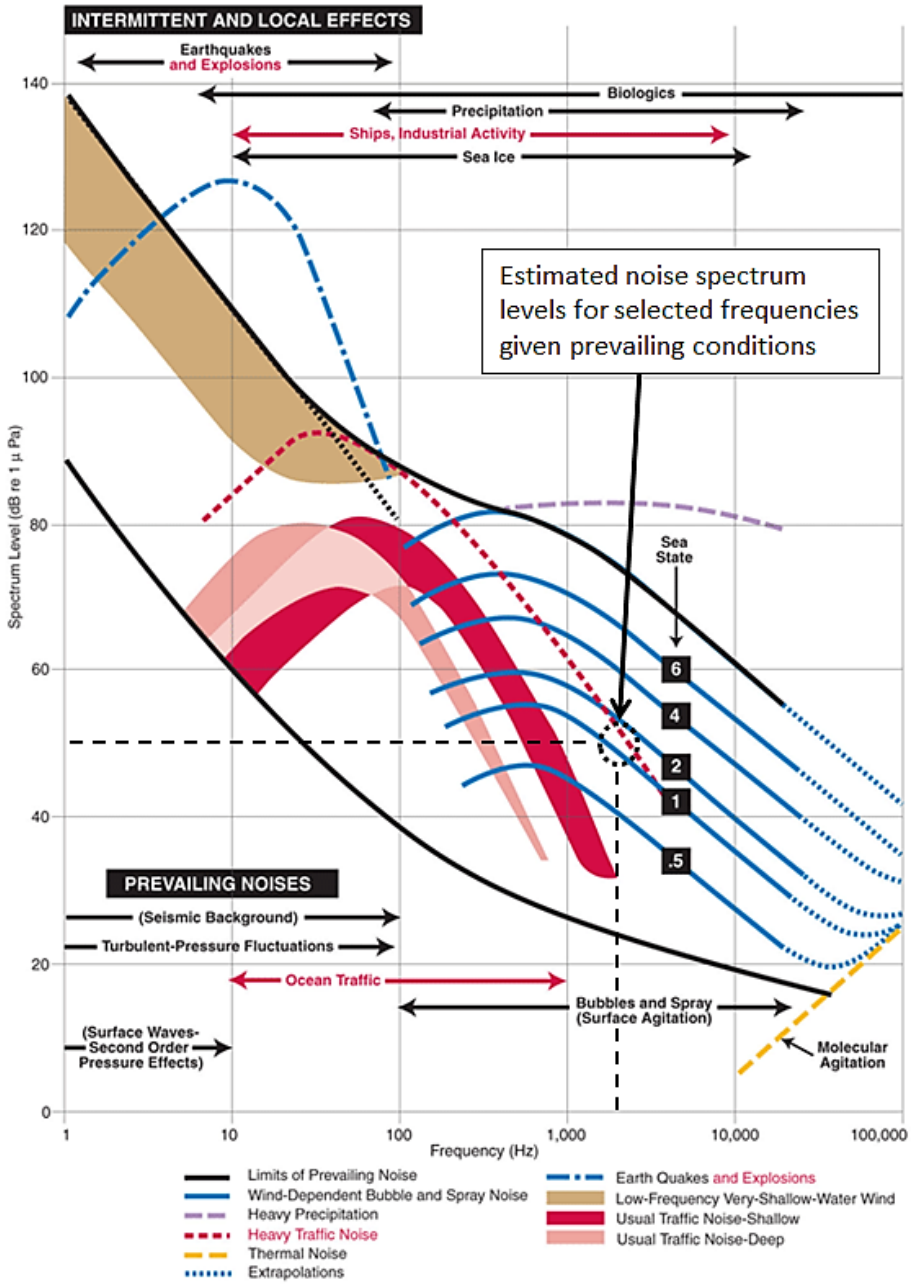

Typical background noise levels in the ocean as adapted from Wenz (1962) by the National Research Council (NRC) in *Ocean Noise and Marine Mammals* (2003) (after Discovery of Sound in the Sea 2015, http://www.dosits.org/science/soundsinthesea/commonsounds/?CFID=3833629&CFTOKEN=32573164)

2. Self-Noise Considerations

The Spray glider is typically a very quiet platform for acoustic sensing. However, several routine onboard operations generate significant self-noise on the recorder. Two mechanical sources are responsible for the majority of this broadband noise: battery pack adjustments and buoyancy engine operation. The glider autopilot controller, with input from flight control dead-reckoning algorithms, commands periodic battery pack movements throughout dives to correct pitch and heading errors (Sherman et al. 2001). Additionally, the coordinated operation of the hydraulic buoyancy pump and battery pack ballast movement is necessary to level off a glide descent.

These sources of noise, common among glider designs, can have a serious impact on acoustic sensing. One solution, implemented aboard a Slocum glider by Rogers et al. (2004), is to have a quiet or "comatose" operating mode available for periods of acoustic data collection. In a similar fashion, the glider used in this study demonstrates the benefits of a silent operating mode during the deep loitering period of its dive cycle. This is because once established at the target depth no further pitch, roll, heading, or depth trim adjustments were necessary. For purpose-built acoustic gliders, careful coordination among acoustic and non-acoustic systems is the ideal solution if systems are to be fully-integrated. In this study, however, the routine self-noise that the Spray glider generates has been carefully identified and ignored using the previously described filtering process.

3. Source-to-receiver Range Estimation

Ambient noise and self-noise were examined to improve the assessment of observed transmission loss. In order to compare this experimentally observed assessment with the Bellhop model predictions it was necessary to estimate glider ranges, from the G34 source, throughout the dive cycle. The experiment was designed to keep the Spray glider at a fairly constant range from the sound source to capture the transition from the shadow zone into the region defined by the reliable acoustic propagation paths.

In reality, environmental factors caused the ranges to vary throughout the experiment. This is due to the drift of the research vessel from wind and currents, as well as the underwater track the glider made between waypoints. While a GPS log aboard the

R/V *Fulmar* provides a good estimate for the sound source drift, the shape of the glider track must be estimated based on two reported surface positions. This is because position updates are not available while the glider is submerged. As previously introduced (see Chapter II), research demonstrates that this deficiency could be solved through coordination with a surface navigation reference such as a GPS-enabled unmanned surface vehicle (USV). Since that capability was not available in this study, the standard mode of Spray glider navigation will be explained.

Before a dive, the Spray glider acquires an initial GPS position and uses a range and heading calculation to path plan to the next waypoint. The planning algorithm does not factor in anticipated drift associated with the depth-averaged ocean currents from previous dive cycles (Sherman et. al 2001). Instead, once the glider is below the surface, navigation accuracy is based on dead-reckoning that is supported with feedback from a 3-dimensional compass (e.g., pitch, roll, and heading) (Sherman et al. 2001). As a result, the GPS fixes that mark where a dive begins and ends are the only available references for the true dive track. While other research has been done to accurately estimate and optimize the underwater path a glider takes (Shim 2009), a simple interpolated straight-line track between the GPS surface fixes will be used here. This assumption is appropriate given the spatial scale of the experiment, as well as the glider's estimate that the depth-averaged currents would help carry it toward its target waypoint.

Additionally, horizontal velocities and their influence on along-track progress for the various phases of the dive are unknown. According to Sherman et al. (2001), Spray glider horizontal velocities are not measured or calculated because they depend on estimates of the angle of attack. As a result, the following assumptions about the dive geometry were made: the glider only made appreciable along-track progress when vertical velocities, and momentum, were highest and not while it loitered at depth; the glider had advanced to approximately the midpoint along the 5.8 km dive-cycle track when it entered its loitering phase. Given these assumptions, estimates were made of along-track glider positions in latitude and longitude that were then paired with the associated dive cycle depths and times. All depths and times which corresponded to the deep loitering period were given the coordinates for the dive cycle halfway point.

THIS PAGE INTENTIONALLY LEFT BLANK

V. RESULTS

Before the unanticipated background noise was filtered out, the raw acoustic pressure data from the Spray glider Acousonde was first examined for the presence of the transmitted signals (see Figure 19). This was accomplished using the previously described LTSA technique (See Chapter IV).

Figure 19. Spectral analysis of glider acoustic data

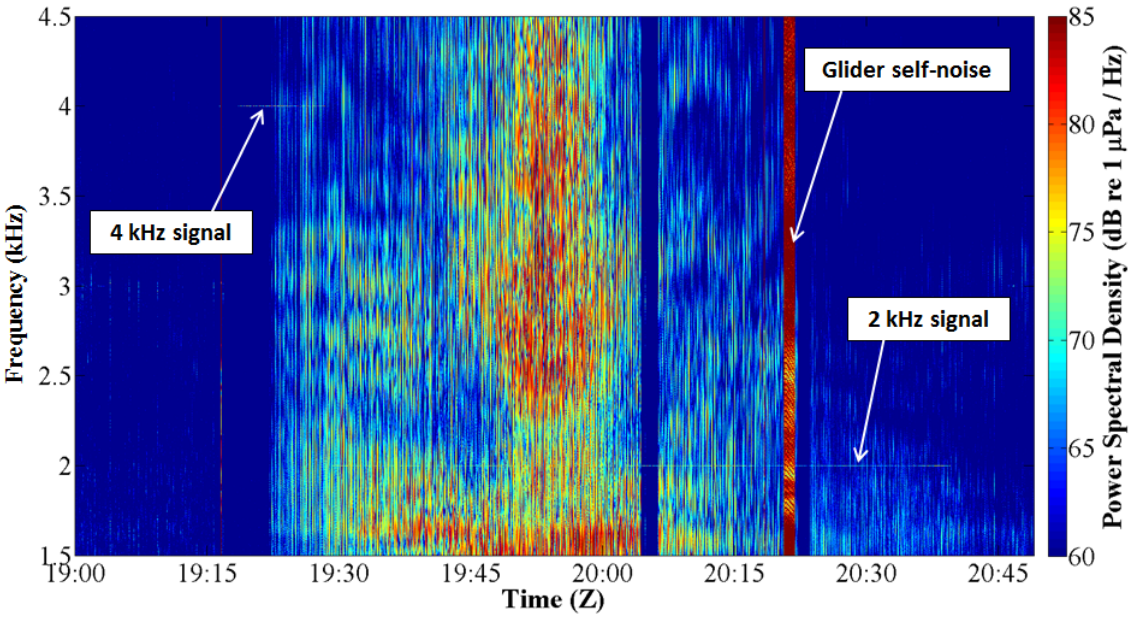

A Long-Term Spectral Average (LTSA) (3 second averaging window, 1 Hz bins, 29 kHz sampling frequency) produced from the Spray glider Acousonde recorder data. The transmitted signals are visible as horizontal traces at 4 kHz and 2 kHz. Geological survey air gun background noise begins during reception of the 4 kHz signal as indicated by the high energy vertical lines. The period of very intense acoustic energy after 20:15 is caused by glider self-noise associated with dive descent level-off procedures.

The output plot clearly shows that the 4 kHz and 2 kHz signals arrived at the Spray glider with sufficient remaining intensity to break out of the background noise. The plot also reveals the relative intensity of the nearby geological survey air gun blasts, as well as glider self-noise associated with the descent level-off. This initial representation of the data provides confirmation that Bellhop model predictions supported the selection of suitable experiment geometry. However, in order to understand how well the model

works as a planning tool it was necessary to compare the acoustic transmission loss predictions to the levels observed during the experiment.

A. TRANSMISSION LOSS COMPARISON

Observed transmission loss was calculated using acoustic source levels and receive levels derived from the G34 and Spray glider Acousonde recorders. Background noise and vehicle self-noise were filtered out of the data set collected aboard the glider. Comparisons were then made with the Bellhop model transmission loss predictions (see Figure 20). To accomplish this, predicted transmission loss values were extracted from the Bellhop model output. The values were selected using glider depths and source-to-receiver range estimates that correspond to the data sample times in the observed data. The final comparison reveals a close agreement with the 4 kHz observations. However, the 2 kHz comparison reveals a bias between the model prediction and field experiment observations. This bias, an average of 5 decibels, is likely due to a slightly different acoustic pressure field structure than what is predicted by the Bellhop model. The range-independent sound speed profile used to generate the Bellhop model prediction is quite possibly the cause for this difference. Nevertheless, the comparison provides suitable confirmation that the model predictions were adequate for planning experiment geometry.

It is interesting to note that the observed transmission loss plot for the 4 kHz signal has variability that occurs at approximately a 10-second period. The hypothesis is that the sea surface swell in the vicinity of the experiment is the cause for this periodic variance in transmission loss. During the experiment, the long-period swell was from the northwest and this resulted in wave crests that were essentially perpendicular to the propagating acoustic energy. Additionally, the Bellhop prediction (see Figure 9) suggests that direct path and surface-reflected path acoustic rays would have been the highest intensity arrivals at the glider location. Therefore, a sea surface with a stable swell period of 10 seconds could certainly have induced periodic acoustic variability in the form of constructive and destructive interference seen at the receiver. Ultimately, the variable

interference is the result of small changes in the acoustic phase and intensity of the primary eigenrays received at the Spray glider.

Figure 20. Observed and predicted transmission loss

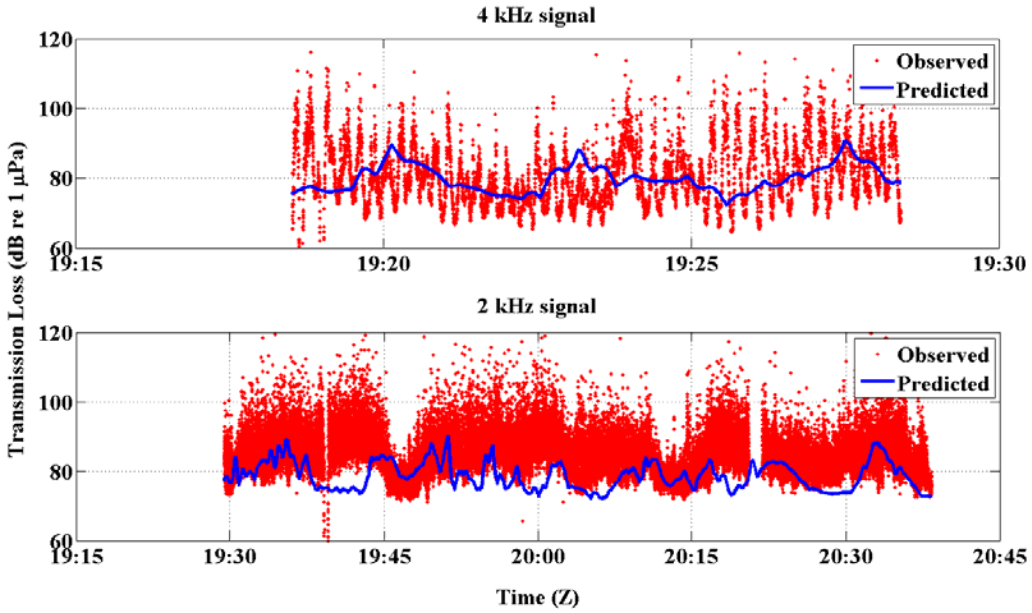

B. LOITER ACOUSTICS

The glider dive cycle conducted during this experiment was planned to incorporate an hour-long loiter at a depth of 1000 meters. While loitering at depth is an advertised capability of current-generation Spray gliders, the process is not optimized for passive acoustic sensing. The acoustic data reveal that operation of the hydraulic buoyancy engine pump , as well as battery pack ballast movement, result in significant self-noise as a loiter is being established (see Figure 21). The selected mounting location for the Acousonde recorder no doubt magnifies this effect. However, once glider self-noise associated with this level-off process subsides the glider is a very quiet platform for passive acoustic sensing. During loitering the 2 kHz signal received at the glider exceeded background noise levels by an average of 12 decibels (see Figure 22).

Figure 21. Self-noise during glider level-off

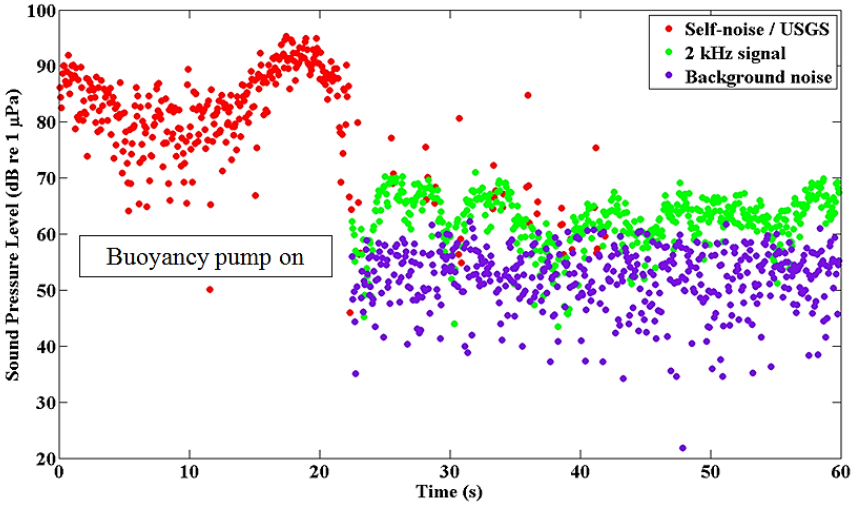

This sample of acoustic data from the Spray glider Acousonde captures the relative intensity of mechanical self-noise produced as the glider established a deep loiter. Noise was identified and filtered from the acoustic pressure data using a MATLAB script. The spectrogram function was then used to transform the pressure data, and sound pressure levels from a 7 Hz wide band centered at 2 kHz were then extracted from the output. The filtered out in-band self-noise and USGS air gun noise is plotted in red. Sound pressure levels from adjacent frequency bands is plotted in purple as a visual representation of background noise and the signal-to-noise ratio (SNR) at the loiter depth.

Figure 22. 2 kHz signal receive level at loiter depth

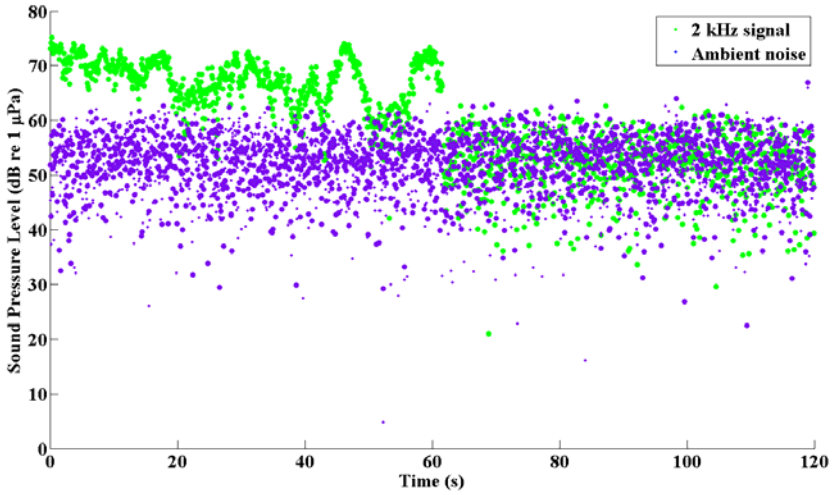

This sample of Spray glider acoustic data depicts reception of the 2 kHz signal shortly before the termination of the deep loiter. Analysis was conducted in the same manner as is described in Figure 21. Acoustic air gun noise has been filtered out and is not shown. Note the in-band receive level of the transmitted 2 kHz signal compared to the ambient noise from adjacent frequency bands. At the 60-second mark the G34 transducer lost power from the shipboard amplifier. The in-band receive level subsequently dropped back down to magnitudes equivalent to the ambient noise.

C. LOITER STABILITY

The Acousonde data reveals that gliders loitering at depth have great potential as persistent acoustic sensing platforms. Separate three-dimensional compass data from the glider dive log also suggests that deep loitering can be very stable. The entire level-off process, from buoyancy pump initiation to approximate equilibrium, required 3.5 minutes. Mechanical processes required in order to establish neutral buoyancy and re-trim pitch and roll account for motion during the first 2 minutes. Vehicle pitch and roll then stabilized after an additional 1.5 minutes. It is useful to mention here that glider pitch attitude settled from 16 degrees nose down in the descent to 23 degrees nose down where it remained throughout the loiter. This is likely due to the loss of lift over the glider's wings as vehicle momentum decreased. Additionally, once the glider had stabilized it slowly drifted 30 meters below the target depth over the duration of the 57 minute loiter.

While vehicle pitch and roll remained fairly constant throughout loitering the vehicle did experience some heading drift. The three-dimensional compass heading information indicates that ocean currents at depth were sufficient to induce a heading drift of approximately one degree per minute. A subsequent glider dive on a reciprocal heading was also examined for comparison. That dive also included a deep loitering period with similar vehicle stability and a heading drift of approximately 6 degrees per minute. These low heading drift values are good indications that a deep-loitering UUV would be a stable platform for both passive acoustic sensing and acoustic communications.

THIS PAGE INTENTIONALLY LEFT BLANK

VI. UNDERWATER ACOUSTIC COMMUNICATIONS

In an unclassified April 2015 presentation at Naval Postgraduate School U.S. Navy Captain Doulas G. Perry, Commander of Submarine Development Squadron FIVE (COMSUBDEVRON 5), presented a list of challenges and needs associated with the integration of unmanned undersea systems. Among the action items on the list he identified two of the fundamental technical limitations associated with UUV operations: high communications latency and data exfiltration alternatives to eliminate vehicle recovery (Perry 2015). These two factors are linked because the faster UUVs can communicate useful data to operational commanders (see Figure 23), the longer autonomous vehicles can persist in the environment where their sensors are needed.

Figure 23. Spray glider with acoustic modem

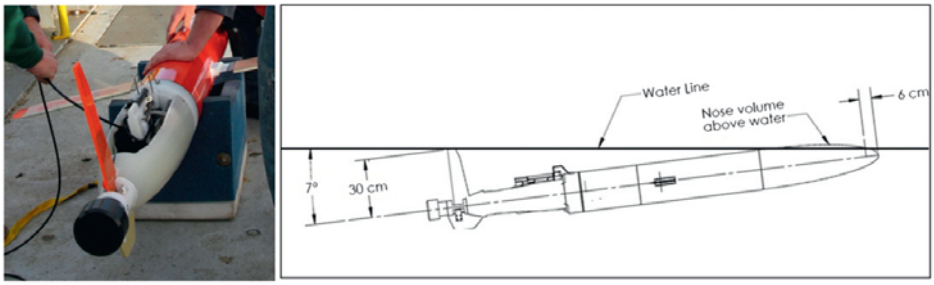

Installation of an acoustic modem transducer (black cylinder) on the tail section of a Spray glider UUV (from Send, U., L. Regier, and B. Jones, 2013: Use of Underwater Gliders for Acoustic Data Retrieval from Subsurface Oceanographic Instruments and Bidirectional Communication in the Deep Ocean. *J. Atmos. Oceanic Technol.*, **30**, 984–998, DOI: 10.1175/JTECH-D-11-00169.1).

In the theoretical network suggested in this study, communication through the ocean surface boundary requires a dedicated gateway USV. The undersea collaboration among distributed autonomous platforms, however, requires a reliable wireless method to connect the network. Established communication methods that utilize the radiofrequency (RF) portion of the electromagnetic spectrum work well in the Earth's atmosphere, but they do not produce adequate results underwater. This is because, compared to sound, RF energy attenuates rapidly in seawater (Urick 1983). As a result, underwater communications using acoustic modems has become the accepted method to achieve

connectivity at practical ranges and depths. However, it is not a perfect solution. The previously discussed factors that impact the propagation of acoustic energy underwater such as sound speed, geometric spreading, and attenuation (see Chapter III) can significantly limit the speed and reliability of acoustic communications. Therefore, it is important to understand how underwater acoustic communications works, and why it can sometimes fail to achieve adequate connectivity.

A. ACOUSTIC DATA TRANSMISSION

An underwater acoustic telemetry modem transmits digital information, or data, through water to a receiver modem using acoustic signals. The transmitting modem encodes, or modulates, a data message to allow for underwater acoustic transmission. The receiving modem then decodes, or demodulates, the incoming signal to reconstruct the original data message (Nortek International 2015). An individual data message is a sequence of symbols, and each symbol is constructed with multiple bits of information (e.g., a binary value of either zero or one). When transmitted, symbols have a particular duration and this determines the number of symbols that are sent per second. Modem output is commonly represented by the rate of data transmission. The number of bits transmitted per second is known as the modem bit rate, and the number of different symbols transmitted per second is referred to as the modem baud rate. Ultimately the performance of the acoustic link between two modems depends on more than just the output of the transmitting modem. The physical behavior of sound in the underwater acoustic channel can limit the rate that symbols are successfully received, known as network throughput.

B. NETWORK THROUGHPUT

The successful reception of underwater acoustic data at a receiving modem is a function of several factors that describe the physical layer of the network. First, transmitted data symbols must travel the required path and distance through the ocean to the receiving modem. Secondly, the symbols must arrive with sufficient signal intensity for recognition above the background noise level. Finally, the receiving modem must be able to demodulate, or decode, the symbols with no errors.

1. Path and Distance

When modulated digital data travels a distance, along a particular network path, to a receiving modem the time delay is known as latency. When data is transmitted in the form of underwater acoustic modem signals, both the acoustic propagation path and the latency are influenced by the change in the physical properties of the ocean along the way (e.g., variations in sound speed). Additionally, the latency is also a function of modem signal encoding and decoding delays. Variability of key physical parameters in the ocean significantly impacts acoustic propagation ranges and affects acoustic travel times. As a result, the latency of an underwater acoustic communications link is quite high by comparison to traditional RF or wired communications networks. Exploitation of underwater direct acoustic propagation paths can minimize travel times and attenuation due to the shorter path distances. However, modem geometry alone cannot completely compensate for the underlying physical limitations of the medium.

2. Signal intensity

When a modem communicates data across an underwater acoustic channel, the signal intensity at the receiving modem is primarily a function of geometric spreading and attenuation. This means that signal intensity decays as communication path lengths increase. As a result, modems must have an ideal separation with respect to range and depth to ensure signals can arrive with sufficient intensity to be decoded. Transmission loss plots, introduced in Chapter IV, are a useful tool to predict the proper geometry that will promote a good signal-to-noise ratio (SNR) at the receiving modem. These plots can be used to estimate the regions of minimal transmission loss for particular acoustic communications frequencies. This is an important consideration to optimize communications because the attenuation of acoustic signals is frequency-dependent: high frequencies can support high data rates but only at shorter ranges, and long range communications are only possible with lower frequencies. This relationship between data rate and frequency is why underwater acoustic communications is commonly referred to as bandwidth-limited. In other words, the bandwidth of acoustic frequencies available for data transmission decreases as range increases. Unfortunately, estimating acoustic

modem performance is more complicated than modeling transmission loss. Reliable underwater acoustic communications also depends on the ability to mitigate the influence of multipath interference.

3. Minimizing error

Given a particular undersea environment, there are many possible combinations of depths and ranges to achieve acoustic communications connectivity between two modems. Optimal connectivity is achieved when a modem can receive, decode, and reconstruct transmitted data symbols with minimal error. In the proposed network, one way to promote this condition is to use a submerged towed body (see Figure 24) to increase the depth of the modem connected to the USV. This will minimize the impact of wind-generated noise, and Doppler motion associated with the moving sea surface. It will also improve connectivity with deep-loitering UUVs that already benefit from an environment of low ambient noise.

Figure 24. Wave Glider SV2 with towed body

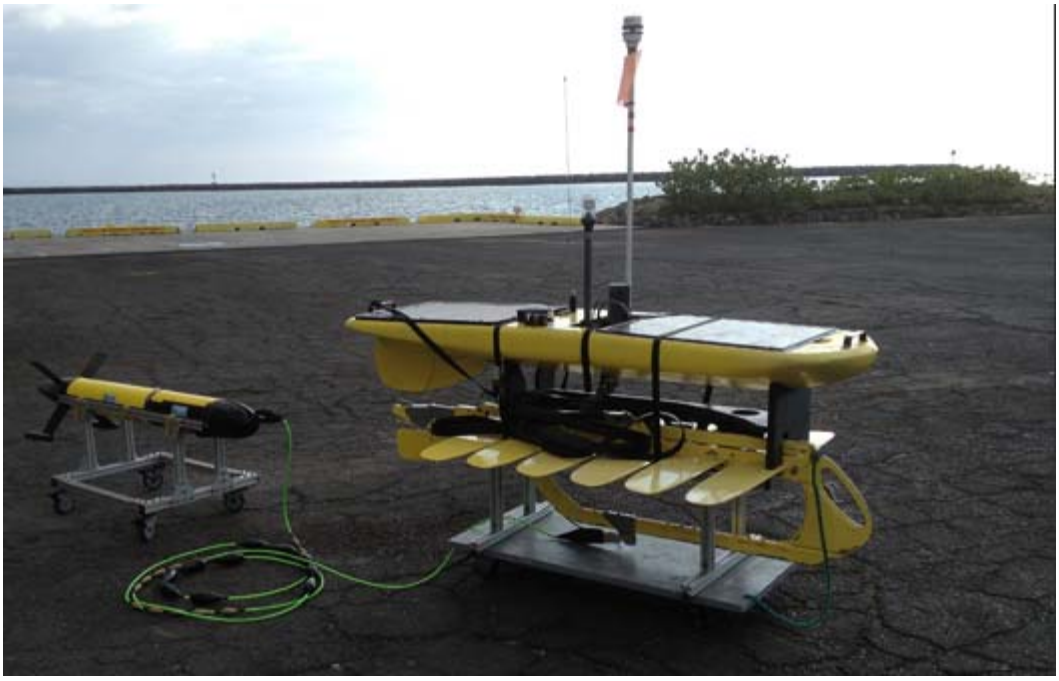

A Liquid Robotics Wave Glider with an underwater towed body that can be outfitted with an acoustic modem (from Integrated Wave Glider-Echosounder. NOAA Fisheries: Northwest Fisheries Science Center, http://www.nwfsc.noaa.gov/news/features/wave_glider/index.cfm).

However, the primary source of error in underwater acoustic communications is multipath interference. Acoustic reflections from the sea surface and ocean bottom result in multiple time-delayed arrivals of the same data symbol. If a modem cannot adapt to the particular time spread between these arrivals then it will not be able to reconstruct an error-free symbol (Send et al. 2013). This condition, known as Intersymbol Interference (ISI), is the reason why it can be challenging to establish reliable acoustic communications in high multipath environments with closely-spaced acoustic arrivals (e.g., shallow water). As a result, the receiving modem will need to request retransmissions of the data. This compensation for high bit error rates is costly in terms of both the time and additional power needed for acoustic transmissions. The degrading effects of ISI are best mitigated in two ways: exploiting direct acoustic propagation paths, and modem signal processing designed to adapt to local conditions.

C. CHANNEL IMPULSE RESPONSE

A common signal processing technique used to improve modem performance involves measuring the impulse response of the acoustic channel between two modems. In signal processing the impulse response of a system is its response to a unit-impulse or brief signal (Johnson 1989). When a modem transmits acoustic signals underwater it results in a sequence of time-delayed arrivals at the receiving modem because of the multipath dispersion of the acoustic energy. The arrivals also vary in amplitude and phase due to ocean surface and bottom reflections. The combined effect at a receiver is time-varying constructive and destructive interference. Given these challenges, acoustic modem manufacturers have developed several techniques to promote successful connectivity.

For example, the Woods Hole Oceanographic Institution (WHOI) Micromodem-2 uses an adaptive decision feedback equalizer (DFE) to automatically respond to variations in the underwater acoustic channel (Gallimore et al. 2010). The equalizer uses received signals to estimate the channel impulse response, and then calculates the equalizer filter weights that will optimize the communication link (Preisig 2005). In addition to adaptive features, manufacturers commonly use forward error correction

(FEC) codes to improve performance (Evologics 2015, Teledyne Benthos 2015). This technique uses specially coded redundant data transmissions that enable a receiving modem to correct errors in received data. As a result, a receiving modem only needs to request retransmission of received data that it is unable to correct. Regardless of the particular technique, all active efforts to mitigate multipath interference reduce the effective bit rate. Therefore, increased acoustic communications reliability comes at the cost of decreased network throughput (Nortek International 2015).

D. EXPERIMENTAL RESULTS

Building a fully-functioning version of the proposed USV/UUV network was not feasible given the constraints of this study. However, it was still vital to demonstrate the previously described acoustic communication concepts in a representative oceanographic environment. To accomplish this, an experiment was conducted to simulate underwater acoustic communications among distributed autonomous platforms. Two acoustic modems were used in the test: one was positioned at various depths to represent a mobile UUV, and a second shallow modem (6 m depth) was deployed at various ranges from the first to simulate a USV gateway platform. A test site in Monterey Bay was chosen with similar bathymetry to the passive acoustic sensing experiment conducted earlier in the year (see Figure 25).

Once again, the Bellhop model and a GDEM-derived sound speed profile were used to produce acoustic propagation predictions. However, this time the incoherent representation of the acoustic pressure field was used to assess the behavior of propagating underwater sound. The incoherent option, when selected, ignores the influence of acoustic phase in order to present a more averaged representation of transmission loss (see Figure 26). This option is appropriate because the precise nature of the acoustic pressure field interference pattern is not useful given modem modulation schemes and the multipath time spread of arrivals (Porter 2011). Instead a simple representation of signal intensity with respect to range and depth is sufficient.

Figure 25. Acoustic communications experiment geometry

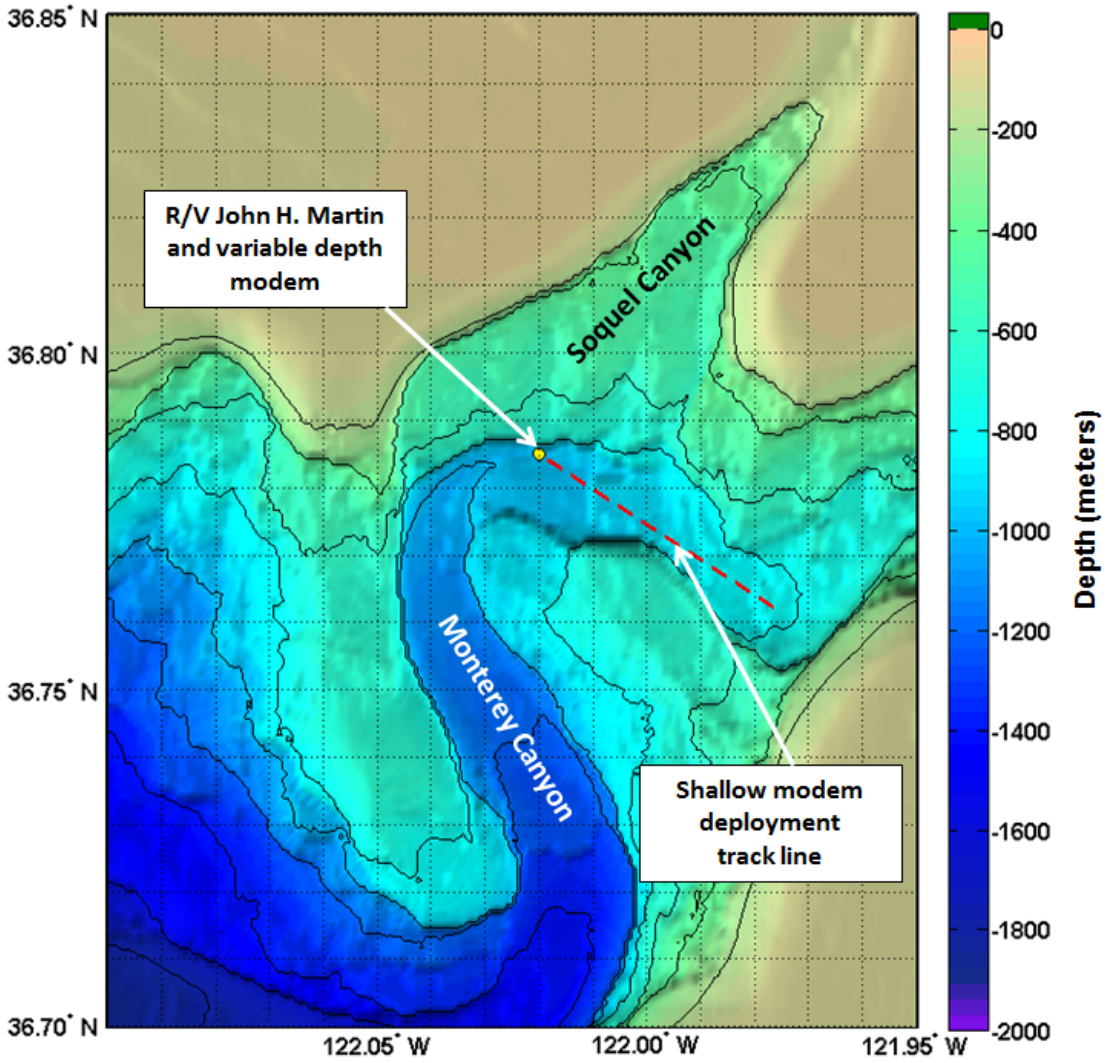

An overhead view of the location and associated bathymetry selected for the acoustic communications experiment conducted on 27 August 2015.

Figure 26. Acoustic modem transmission loss prediction

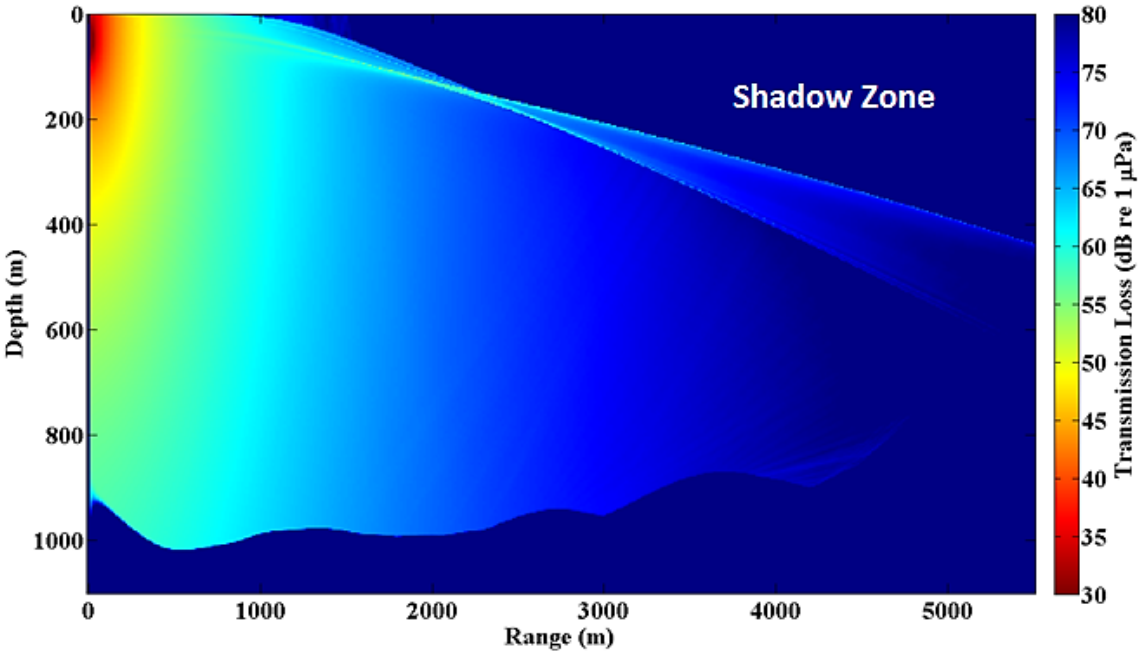

An incoherent transmission loss prediction for an acoustic modem signal centered at 14 kHz. The plot is useful for identification of regions where signal intensity should promote reception. However, even with sufficient signal intensity above the background noise modems must also be able to mitigate the influence of multipath interference.

Observations from this experiment, at several combinations of ranges and depths, resulted in connectivity between the modems. When the modems were able to successfully communicate, their geometry was consistent with the regions of lower predicted transmission loss. As expected, communication was ineffective when one modem was located in the region of the plot that depicts the acoustic shadow zone. In several instances, when connectivity issues were believed to be the result of multipath interference, a change in depth separation between the modems was enough to improve communications. The estimated acoustic ray paths and channel impulse response for two representative scenarios from the field test are presented in the following figures (see Figures 27, 28, 29, and 30). The method for plotting the Bellhop acoustic ray amplitude delay information is derived from Torres (2007).

Figure 27. Multipath arrivals for geometry that supported connectivity (source at 250 m, receiver at 6 m)

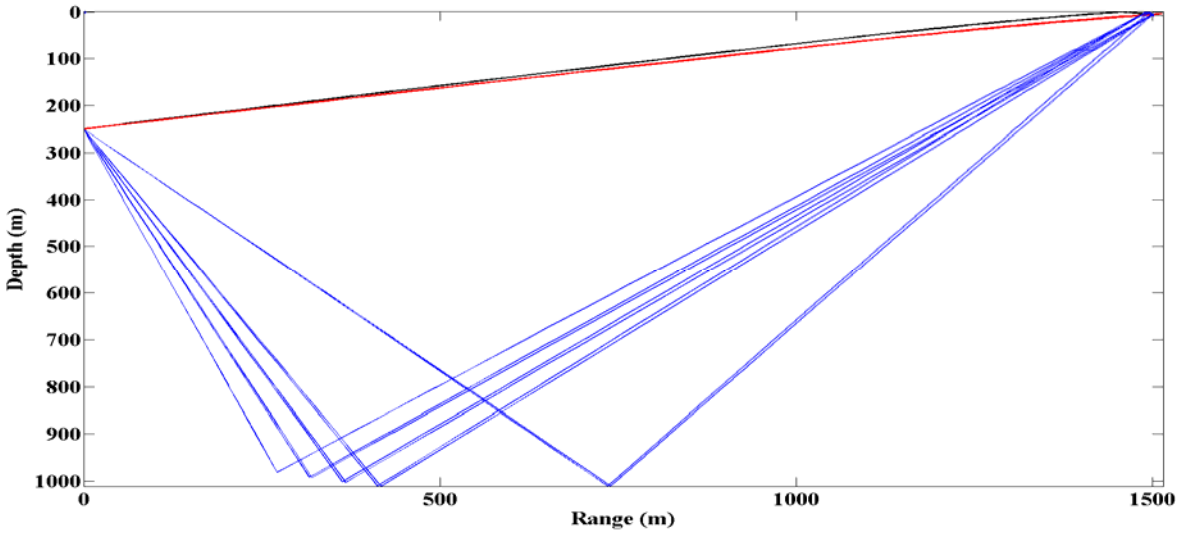

A Bellhop eigenray plot that depicts estimated acoustic ray paths between modems for a geometry that resulted in excellent connectivity during the field test. The red line is the direct path, the black line indicates a path with a single boundary interaction (surface reflection), and the blue lines represent bottom-reflected ray paths.

Figure 28. Channel Impulse response (source at 250 m, receiver at 6 m)

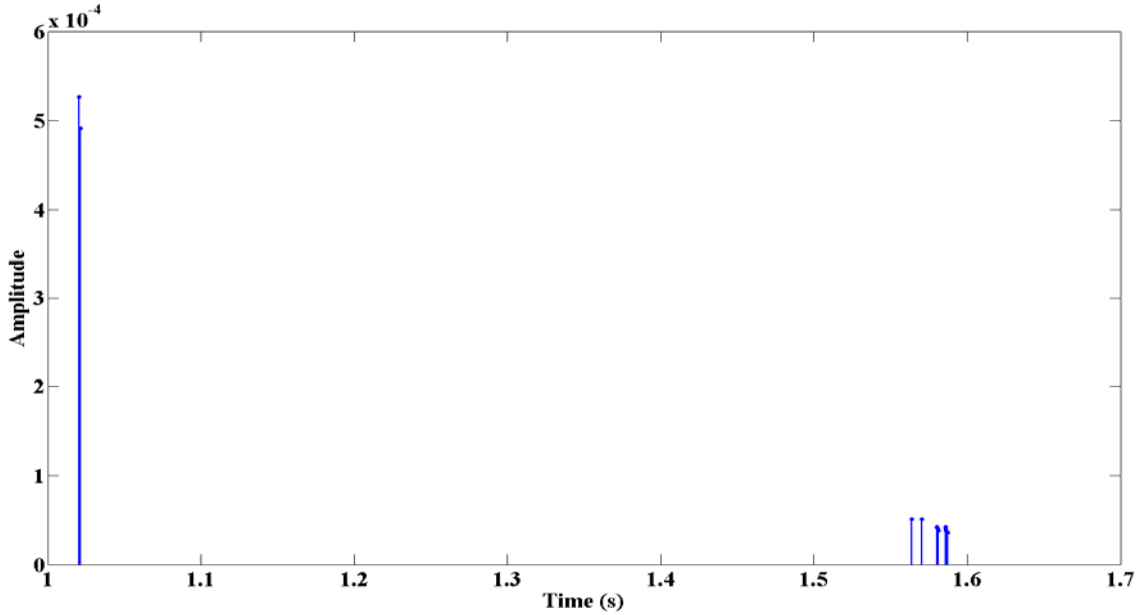

Multipath arrival time delays (horizontal axis) and dimensionless amplitudes (vertical axis) from a Bellhop acoustic channel impulse response prediction. The plot is an estimate of the arrivals seen at the receiver for the most favorable acoustic modem geometry tested during the experiment (source at 250 m transmitting to a receiver at 6 m).

Figure 29. Multipath arrivals for geometry that did not support connectivity (source at 50 m, receiver at 6 m)

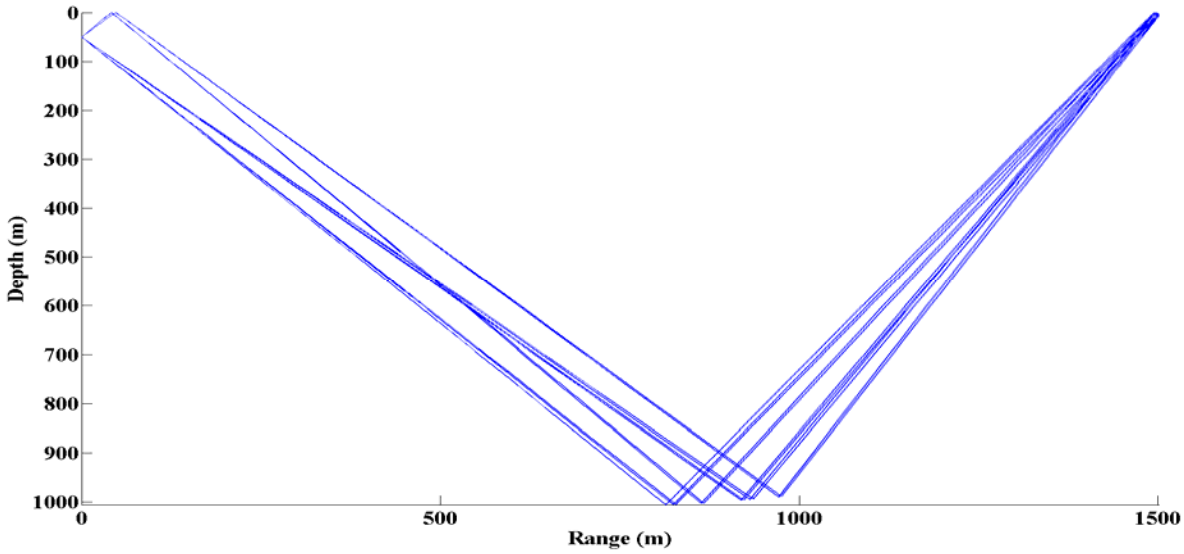

A Bellhop eigenray plot that depicts estimated acoustic ray paths between modems for a geometry that did not result in successful modem communications during the field test. Note the lack of direct acoustic propagation paths in the prediction.

Figure 30. Channel impulse response (source at 50 m, receiver at 6 m)

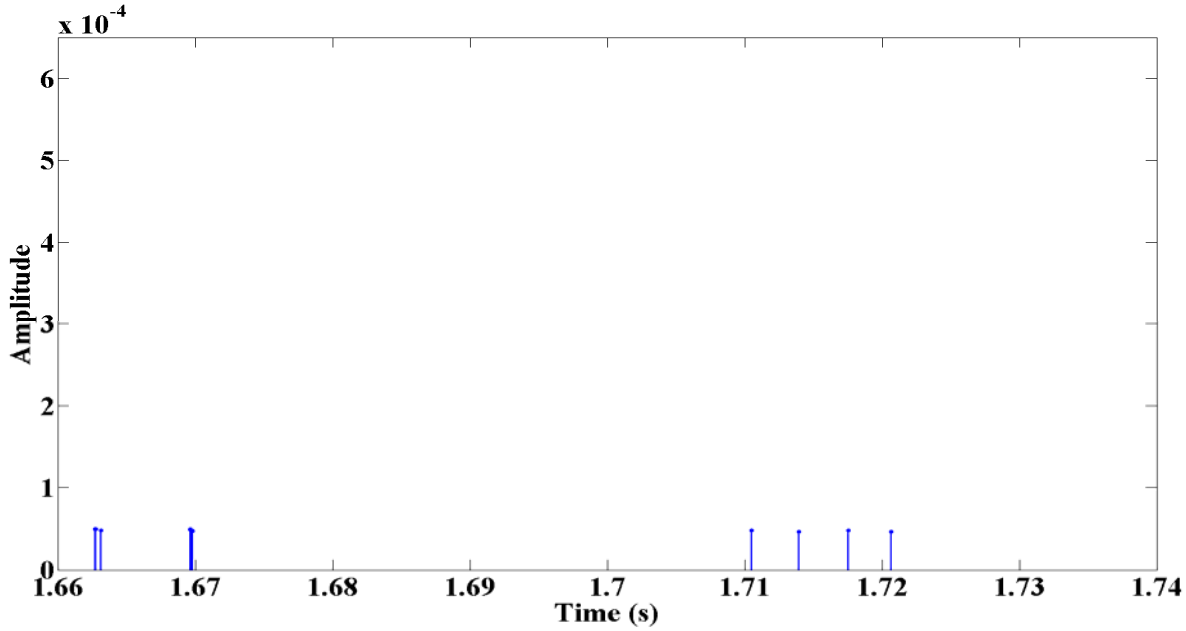

Predicted acoustic multipath arrival time delays and amplitudes for a modem separation that did not allow for any successful communications during the field test. Note the amplitudes and time spread of arrivals compared to Figure 28.

These observations suggest that it should be possible to predict modem geometry that will promote optimal acoustic communications given the unique parameters of a particular underwater acoustic channel. Therefore a logical addition to the proposed USV/UUV system is to develop a real-time network connectivity model to optimize acoustic communications (Horner and Xie 2012). Ideally, the model would run aboard the USV and utilize in-situ oceanographic observations to better tune network communications to the local environment.

E. POWER REQUIREMENTS

While the underwater environment imposes significant limitations on acoustic communications, the most important limiting factor for battery-operated UUVs is power. Acoustic communications requires power for both receive and transmit modes. However, the amount of power that is required to operate a modem transducer for acoustic transmissions is much more than is needed for a passive receive mode (Send et al. 2013). For example, the LinkQuest UWM3000H has an advertised maximum operating range of 6000 meters with receive mode and transmit mode power requirements of 0.8 watts and 12 watts, respectively (LinkQuest Inc. 2015). While this particular modem might not be the best choice for a glider UUV the listed specifications reinforce the relationship between power consumption and working range. Additionally, a quick survey of modem designs reveals that increased ranges also require larger acoustic transducers and consequently a larger modem form factor. This means that there is no one size fits all solution. Regardless of the modem, acoustic transmit power requirements will require a significant share of the power budget. While this is not a concern for a USV that can use solar energy to replenish its power supply, a battery-operated glider UUV must be carefully designed to communicate in a power-efficient manner. This constraint makes a deep glider loiter, that limits ballast movement and buoyancy engine pumping, an even more appealing aspect of the proposed network model.

F. IMPROVING PERFORMANCE

Despite the factors that influence the reliability of acoustic communications there are still many ways to encourage consistent levels performance. Broadly speaking,

performance improvements can be broken down into three categories: hardware and design, software, and message prioritization.

1. Hardware and Design Features

Two common examples of how to improve underwater acoustic modem performance are to utilize directional transducers and acoustic baffles (LinkQuest Inc. 2015, Nortek International 2015). A directional transducer sends and receives acoustic signals over a limited range of bearings in order to focus signal intensity in the direction of a particular receiver. Directional transmissions can be especially useful for limiting multipath interference when the relative bearing to an intended receiving modem is known. Acoustic baffles are design features of modem installation that are used to physically block reception of acoustic arrivals from undesired directions. Additionally, a network design feature that has potential to improve connectivity is the use of purpose-built relay node UUVs. A vehicle specifically designed to loiter and relay data would extend communications ranges and allow distributed assets to connect with the surface gateway USV at greater ranges.

2. Software

The previously described acoustic communications experiment highlights the value of implementing onboard network connectivity models to optimize communications. The probability that the proposed network would remain connected ultimately depends on the optimal use of acoustic communications for given environmental conditions. Acoustic channel simulators that could predict both individual modem performance, as well as the performance of the greater network, would be a very useful tool to support network autonomy.

Performance gains can also be realized through the use of separate models to plan sensor employment. This need for multiple models is necessary because optimal communications ranges and sensor coverage ranges will not always be similar. As a result, the network will need a computational method that can strike a balance between connectivity and sensor coverage.

3. Message Prioritization

Acoustic modem transmissions require a large share of a battery-operated UUVs power budget. It is also not feasible to transmit all sensor data due to the bandwidth and data rate limitations imposed by the underwater acoustic channel. Therefore, acoustic communications should be prioritized in order to maximize vehicle endurance. Several message types will be required on a routine basis, but they will each have their own unique intervals. Some examples of necessary messages include contact reports, navigation updates, raw sensor data samples, C2 instructions, and vehicle health monitoring status updates. Given the variety of desired information, it might be very useful to explore ways to simplify acoustic messages and establish an optimal hierarchy for transmissions.

THIS PAGE INTENTIONALLY LEFT BLANK

VII. CONCLUSION

Experimental results from this study demonstrate that ocean glider Unmanned Undersea Vehicles (UUVs) are effective mobile platforms to support persistent acoustic sensing. Additionally, observations and background research suggest that underwater acoustic communications is a feasible method to connect an unmanned surface vehicle (USV) and a submerged glider UUV.

During a passive acoustic sensing test a medium frequency acoustic source was deployed at a range of 5.5 km from a receiver on board a Spray glider UUV conducting a 1000 m dive. Transmitted acoustic signals were successfully received while the glider was in motion, and reception improved during a quiet 1000 m loitering period. Acoustic propagation modeling supported the selection of experiment geometry that successfully demonstrated the value of a mobile sensing platform: gliders can adapt to local environmental conditions in order to exploit acoustic energy that propagates along the reliable acoustic path (RAP). It was also noted that deep UUV loiters are operating regimes that exhibit low platform self-noise and have the potential to be very stable. It is easy to see how this stability can be leveraged to maximize time on station and sensor coverage area.

A separate acoustic communications experiment was conducted in similar environmental conditions to simulate communications among distributed autonomous platforms. Two acoustic modems were utilized in order to represent a UUV at various loitering depths, as well as a surface gateway USV. Results confirm that modem ranges and depths that promote ideal communications can be effectively predicted with in-situ observations of oceanographic parameters. However, in future applications the ability to maintain optimal modem geometry, as well as manage power requirements will be primary performance constraints.

A. RECOMMENDATIONS

If networks of autonomous gliders are to function effectively in remote operating areas, with limited human oversight, they will need to have the ability to conduct critical signal processing tasks onboard. While post-processing of sensor data was acceptable for the demonstration in this study, it is not the ideal approach for the proposed network. A submerged vehicle will not be able to communicate a large quantity of raw sensor data over appreciable ranges in a timely fashion. Providing vehicles with organic signal detection, classification, and localization capabilities should be the top priority for future design efforts. Additionally, onboard signal processing routines need to utilize available power and internal data storage capacity efficiently in order to take advantage of the long-endurance of glider USV/UUV platforms.

Research should also continue to consider ocean glider platforms for deep loitering. The more physically benign environment of the deep ocean is a better environment for passive acoustic sensing and acoustic communication to surface platforms. Increased depths also inhibit the bio fouling that leads to undesirable hydrodynamic drag and degraded performance. In order to enable this manner of operational use, it will be necessary to provide updated navigational information to submerged vehicles. We feel this is one of the more critical areas of focus for future research efforts.

B. FUTURE PLATFORM CHARACTERISTICS

In addition to onboard low-power signal processing future platforms designed to support the proposed network should have the following characteristics. First, vehicles should have onboard numerical models that use in-situ observations to improve prediction efforts. These models are necessary in order to optimize sensor placement and promote acoustic communications connectivity. Consideration should be given to running such models aboard the USV to take advantage of the renewable power supply. Naturally, given the battery-powered nature of current glider UUVs, onboard processing and modelling will greatly benefit from future advancements in power cell design and in-field recharging capabilities.

Secondly, the USV gateway platform should be able to provide navigation updates to each of the distributed UUVs under its control using underwater acoustic communications. This will allow glider UUVs to minimize trips to the surface and allocate more of their power budget to onboard sensors, signal processing, and data off-boarding via acoustic communications. However, as a backup capability, glider UUVs should still retain the option to conduct traditional surfacing for communication and navigation updates. This is necessary in order to mitigate the risks associated with a catastrophic loss of the network gateway USV due to a ship strike, storm, or interception.

Finally, efforts to improve acoustic sensors should focus on reducing power, size, and weight requirements. Vector sensors and small volumetric arrays should be investigated for use aboard platforms tasked with passive acoustic sensing. Given their compact size, as well as the ability to resolve bearings to an acoustic source, these sensors would add great flexibility to a sensing network. If individual UUV platforms could resolve the location of an acoustic signal then it might be possible to reduce the required number of sensing nodes in a distributed network.

THIS PAGE INTENTIONALLY LEFT BLANK

APPENDIX A. BELLHOP INPUT ENVIRONMENTAL FILE

```
'Spray Prediction SSP ext. w/GDEM, 10 m interpolation)' ! TITLE
2000.0               ! FREQ (Hz)
1                    ! NMEDIA
'SVWT'               ! (SSP spline, surf. vacuum,dB/wavelength, Thorpe)
51  0.0    1261      ! DEPTH of bottom (m)
    0.0    1504.62 /
    0.8    1504.62 /
   10.8    1504.00 /
   20.8    1504.06 /
   30.8    1504.17 /
   40.8    1497.12 /
   50.8    1493.58 /
   60.8    1490.78 /
   70.8    1489.76 /
   80.8    1488.80 /
   90.8    1488.18 /
  100.8    1488.14 /
  110.8    1488.04 /
  120.8    1487.95 /
  130.8    1487.57 /
  140.8    1487.16 /
  150.8    1486.99 /
  160.8    1487.28 /
  170.8    1487.28 /
  180.8    1487.23 /
  190.8    1487.01 /
  200.8    1486.98 /
  210.8    1486.91 /
  220.8    1486.76 /
  230.8    1486.70 /
  240.8    1486.25 /
  250.8    1486.01 /
  260.8    1486.67 /
  270.8    1486.10 /
  280.8    1485.94 /
  290.8    1485.43 /
  300.8    1485.42 /
  310.8    1485.56 /
  320.8    1485.28 /
  330.8    1484.76 /
  340.8    1483.75 /
  350.8    1483.77 /
  360.8    1483.13 /
  370.8    1483.03 /
  380.8    1482.77 /
  390.8    1482.45 /
  400.8    1482.45 /
  410.8    1482.54 /
  420.8    1482.81 /
  430.8    1482.77 /
  440.8    1482.44 /
```

```
450.8    1482.28 /
460.8    1482.00 /
470.8    1481.88 /
480.8    1481.86 /
490.8    1481.95 /
500.8    1481.89 /
510.8    1481.57 /
520.8    1481.64 /
530.8    1481.25 /
540.8    1481.36 /
550.8    1480.97 /
560.8    1480.92 /
570.8    1481.08 /
580.8    1481.37 /
590.8    1481.53 /
600.8    1481.63 /
610.8    1481.67 /
620.8    1481.61 /
630.8    1481.50 /
640.8    1481.64 /
650.8    1481.80 /
660.8    1481.92 /
670.8    1481.73 /
680.8    1481.41 /
690.8    1481.35 /
700.8    1481.37 /
710.8    1481.40 /
720.8    1481.35 /
730.8    1481.40 /
740.8    1481.33 /
750.8    1481.28 /
760.8    1481.19 /
770.8    1481.12 /
780.8    1481.20 /
790.8    1481.28 /
800.8    1481.27 /
810.8    1481.29 /
820.8    1481.24 /
830.8    1481.18 /
840.8    1481.29 /
850.8    1481.30 /
860.8    1481.30 /
870.8    1481.30 /
880.8    1481.24 /
890.8    1481.22 /
900.8    1481.25 /
910.8    1481.36 /
920.8    1481.29 /
930.8    1481.42 /
940.8    1481.56 /
950.8    1481.72 /
960.8    1481.86 /
970.8    1481.83 /
980.8    1481.92 /
990.8    1481.95 /
```

```
 1000.8    1481.94 /
 1010.8    1482.05 /
 1020.8    1482.11 /
 1030.8    1482.13 /
 1040.8    1482.16 /
 1050.8    1482.19 /
 1060.8    1482.21 /
 1070.8    1482.24 /
 1080.8    1482.27 /
 1090.8    1482.29 /
 1100.8    1482.32 /
 1110.8    1482.39 /
 1120.8    1482.46 /
 1130.8    1482.53 /
 1140.8    1482.60 /
 1150.8    1482.66 /
 1160.8    1482.73 /
 1170.8    1482.80 /
 1180.8    1482.87 /
 1190.8    1482.94 /
 1200.8    1483.01 /
 1210.8    1483.09 /
 1220.8    1483.17 /
 1230.8    1483.25 /
 1240.8    1483.33 /
 1250.8    1483.41 /
 1260.8    1483.48 /
 1261.0    1483.80 /
'A*'   0.0
1261 1503.0 0.0 1.352 0.1458    /
1                      ! NSD
25.0 /               ! SD(1:NSD) (m)
1600                    ! NRD
0.0 1500 /                 ! RD(1:NRD) (m)
1600                     ! NR
0.0 8 /                  ! R(1:NR) (km)
'CB'                    ! 'R/C/I/S'
0                    ! NBeams
-90.0 90.0 /           ! ALPHA1,2 (degrees)
0.0 1500.0 8.0       ! STEP (m), ZBOX (m), RBOX (km)
```

Notes on Bottom parameters: the ocean bottom is modeled as an acoustic half-space and the range-dependent bathymetry file described in Chapter IV is called on the same line (`'A*'`). The subsequent parameters indicate depth of the bottom (1261 m), compressional sound speed of the bottom sediment (1503 m/s), bottom type density (1.352 gm/cm^3), and bottom type attenuation coefficient (0.1458 dB/λ).

The bottom type (Hemipelagic Terrigenous Clay) is derived from the Bottom Sediment Type (BST) database maintained by the U.S. Naval Oceanographic Office Acoustics Division as part of the U.S. Navy Oceanographic and Atmospheric Master Library (OAML). The additional bottom geo-acoustic parameters are estimates based on empirically derived dependencies (Hamilton 1980, Hamilton and Bachman 1982).

APPENDIX B. ACOUSONDE SETTINGS

Spray glider Acousonde

Serial Number	B003A044 (Spray glider)
Channel	1 (Low Power)
Sampling Frequency	29,038 kHz
Cutoff Frequency	9,292 kHz
Total path gain (antialiasing filter engaged)	+22.5 dB
High-pass filter cutoff frequency	22 Hz
Sensitivity after preamplification	-187.3 dB re 1 V/micro Pa

G34 source monitor Acousonde

Serial Number	B003A011 (G34 source monitor)
Channel	1 (Low Power)
Sampling Frequency	29,038 kHz
Cutoff Frequency	9,292 kHz
Total path gain (antialiasing filter engaged)	+2.4 dB
High-pass filter cutoff frequency	38 Hz
Sensitivity after preamplification	-188.1 dB re 1 V/micro Pa

THIS PAGE INTENTIONALLY LEFT BLANK

LIST OF REFERENCES

Acoustimetrics, 2015: Acousonde 3A Brochure with specifications. [Available online at http://www.acousonde.com/downloads/Acousonde3A_Brochure.pdf]

Baumgartner, M. F., K. M. Stafford, P. Winsor, H. Statscewich, and D. M. Fratantoni, 2014: Glider-Based Passive Acoustic Monitoring in the Arctic., *Mar. Technol. Soc. J.*, **48**, 5, 40–51.

Bingham, B., N. Kraus, B. Howe, L. Freitag, K. Ball, P. Koski, and Eric Gallimore, 2012: Passive and Active Acoustics Using an Autonomous Wave Glider., *J. Field Robot.*, **29**, 6, 911–923, doi: 10.1002/rob.21424.

Brekhovskikh, L. M., and Yu. P. Lysanov, 2003: *Fundamentals of Ocean Acoustics*. Springer, 280 pp.

Dassatti, A., M. van der Schaar, P. Guerrini, S. Zaugg, L. Houegnigan, A. Maguer, and M. Andre, 2011: On-board Underwater Glider Real-time Acoustic Environment Sensing., *IEEE*, doi: 10.1109/Oceans-Spain.2011.6003482.

Dol, H. S., M. E. G. D. Colin, M. A. Ainslie, P. A. van Walree, and J. Janmaat, 2013: Simulation of an Underwater Acoustic Communication Channel Characterized by Wind-Generated Surface Waves and Bubbles. *IEEE J. Ocean. Eng.*, **38(4)**, 642 – 654, doi: 10.1109/JOE.2013.2278931.

Evologics, 2015, Evologics Underwater Acoustic Modems product information guide. [Available online at http://www.evologics.de/files/DataSheets/EvoLogics_S2CR_Modems_a4_WEB.pdf]

Fofonoff, P., and Millard, R.C. Jr, 1983: Algorithms for computation of fundamental properties of Seawater. Unesco technical papers in marine science, No. 44, 58 pp. [Available online at http://unesdoc.unesco.org/images/0005/000598/059832eb.pdf]

Francois, R. E., and G. R. Garrison, 1982: Sound absorption based on ocean measurements. Part II: Boric acid contribution and equation for total absorption. *J. Acoust. Soc. Am.*, **72**, 6, 1879–1890.

Gallimore, E., J. Partan, I. Vaughn, S. Singh, J. Shusta, and L. Freitag, 2010: The WHOI Micromodem-2: A Scalable System for Acoustic Communications and Networking. *IEEE Oceans September 2010 Seattle, WA.* 7 pp. DOI: 10.1109/OCEANS.2010.5664354.

Hamilton, E. L., 1980: Geoacoustic Modeling of the sea floor. *J. Acoust. Soc. Am.*, **68(5)**, 1313-1340.

Hamilton, E. L., and R. T. Bachman, 1982: Sound velocity and related properties of marine sediments. *J. Acoust. Soc. Am.*, **72(6)**, 1891-1904.

Horner, D., and G. Xie, 2012: Undersea acoustic communication maps for collaborative navigation. Autonomous Underwater Vehicles (AUV) IEEE/OES Conference September 2012, Southampton. 7 pp. DOI: 10.1109/AUV.2012.6380757.

Hovem, J. M., 2013: Ray trace modeling of underwater sound propagation. *Modeling and Measurement Methods for Acoustic Waves and for Acoustic Microdevices*, M. G. Beghi, Ed., InTech, DOI: 10.5772/55935.

Howe, B. M., Y. Chao, P. Arabshahi, S. Roy, T. McGinnis, and A. Gray, 2010: A Smart Sensor Web for Ocean Observation: Fixed and Mobile Platforms, Integrated Acoustics, Satellites and Predictive Modeling., **3**, 4, 507–521.

Hughes, D. T., F. Baralli, S. Kemna, M. Hamilton, A. Vermeij, 2009: Collaborative multistatic ASW using AUVs: demonstrating necessary technologies. Maritime Systems and Technology Conference, NATO Undersea Research Centre. [Available at http://www.nurc.nato.int/]

Jenkins, S. A., D. Humphreys, J. Sherman, J. Osse, C. Jones, N. Leonard, T. Clem, J. Berry, and J. Wasyl, 2003: Underwater Glider System Study. Technical report, Office of Naval Research.

Johnson, J.R., 1989: *Introduction to Digital Signal Processing*, Prentice Hall, 407 pp.

Joseph, J. E., D. Horner, 2014: Integration and Optimization of UUV/USV Operations in Environmental Characterization, unpublished N2/N6 approved NPS research proposal.

LinkQuest Inc., 2015: LinkQuest Underwater Acoustic Modems UWM3000H Specifications. [Available online at http://www.link-quest.com/html/uwm3000h.htm]

Llor, J., and M. P. Malubres, 2013: Statistical Modeling of Large-Scale Signal Path Loss in Underwater Acoustic Networks. *Sensors 2013*, **13(2)**, 2279-2294, doi:10.3390/s130202279

Maher, Norman, and F. L. Wong, 2001: Low-resolution (250-m) gridded bathymetry and shaded relief image (CCALBATG, CCALSHD.TIF) of the region offshore of central California between Point Reyes and San Simeon. [Available online at http://geopubs.wr.usgs.gov/open-file/of01-179]

Maguer, A., R. Dymond, A. Grati, R. Stoner, P. Guerrini, L. Troiano, and A. Alvarez, 2013: Ocean gliders payloads for persistent maritime surveillance and monitoring., *NATO Centre for Maritime Research and Experimentation (CMRE)*, 8 pp.

McGillivary, P., J. Borges de Sousa, R. Martins, K. Rajan, and F. Leroy, 2012: Integrating Autonomous Underwater Vessels, Surface Vessels and Aircraft as Persistent Surveillance Components of Ocean Observing Studies., *Southampton, UK, 2012 IEEE/OES*, doi: 10.1109/AUV.2012.6380734.

Miller, C., 2013: Acousonderead (MATLAB script) [Available at http://www.acousonde.com/downloads.html]

Morgan, P., and L. Pender, 2003: Sound Velocity in Seawater (SW_SVEL.m) [Available as part of the Mixing (MX) Oceanographic Toolbox for EM-APEX float data at http://www.mathworks.com/matlabcentral/fileexchange/47595-mixing--mx--oceanographic-toolbox-for-em-apex-float-data]

Nortek International, 2015: Acoustic Modem. [Available online at http://www.nortek-as.com/en/service/deployment-assesories/acoustic-modem]

Perry, D. G., 2015. Autonomous vehicle presentation given at Naval Postgraduate School, unpublished.

Porter, M. B., 2011: The Bellhop manual and user's guide preliminary draft. Heat, Light, and Sound Research, Inc. [Available online at http://oalib.hlsresearch.com/Rays/]

Porter, M.B., and H. P. Bucker, 1987: Gaussian beam tracing for computing ocean acoustic fields. *J. Acoust. Soc. Am.*, **82**, 4, 1349-1359.

Preisig, J. C., 2005: Performance analysis of adaptive equalization for coherent acoustic communications in the time-varying ocean environment. *J. Acoust. Soc. Am.*, **118(1)**, 263-278, DOI: 10.1121/1.1907106.

Rayleigh, J. W. S., 1894: *The Theory of Sound*. Macmillan and Co. 480 pp.

Rogers, E. O., J. G. Gunderson, W. S. Smith, G. F. Denny, and P. J. Farley, 2004: Underwater Acoustic Glider., *Geoscience and Remote Sensing Symposium IEEE*, 2241–2244.

Rudnick, D. L., R.E. Davis, C. C. Eriksen, D. M. Fratantoni, and M. J. Perry, 2004: Underwater Gliders for Ocean Research., *Mar. Technol. Soc. J.*, **38**, 2, 73–84.

Send, U., L. Regier, and B. Jones, 2013: Use of Underwater Gliders for Acoustic Data Retrieval from Subsurface Oceanographic Instruments and Bidirectional Communication in the Deep Ocean. J. Atmos. *Oceanic Technol.*, **30**, 984-998, DOI: 10.1175/JTECH-D-11-00169.1

Sherman, J., R. E. Davis, W. B. Owens, and J. Valdes, 2001: The Autonomous Underwater Glider "Spray.," *IEEE J. Ocean. Eng.*, **26**, 4, 437–446.

Shim, J. E., 2009: Optimal estimation of glider's underwater trajectory with depth-dependent correction using the Navy Coastal Ocean Model with application to antisubmarine warfare. M. S. Thesis, Dept. of Oceanography, Naval Postgraduate School, 166 pp.

Scripps Whale Acoustic Lab, 2015: Long-Term Spectral Average (LTSA). [Available online at http://cetus.ucsd.edu/technologies_LTSA.html]

Stanway, M. J., B. Kieft, T. Hoover, B. Hobson, A. Hamilton, and J. Bellingham, 2014: Acoustic Tracking and Homing with a Long-Range AUV., 7 pp., doi: 10.1109/OCEANS.2014.7003277.

Stoica, P., and R. Moses, 2005: *Spectral Analysis of Signals*. Prentice Hall, 452 pp.

Thompson, S. R., 2009: Sound Propagation Considerations for a Deep-Ocean Acoustic Network. M. S. Thesis, Dept. of Physics, Naval Postgraduate School, 64 pp.

Teledyne Benthos, 2015: Benthos Acoustic Modems brochure. [Available online at https://teledynebenthos.com/_doc/main/Brochures_Datasheets/Modems_brochure_2013_2014_lo.pdf]

Teledyne Webb Research, 2015: Slocum G2 Glider Data Sheet. [Available online at http://www.webbresearch.com/pdf/Slocum_Glider_Data_Sheet.pdf]

Torres, J. C., 2007: Modeling of High-frequency Acoustic Propagation in Shallow Water. M. S. Thesis, Dept. of Physics, Naval Postgraduate School, 150 pp.

Urick, R. J., 1983: *Principles of Underwater Sound:* Third Edition. Peninsula Publishing, 423 pp.

U.S. Department of the Navy, 2004: The Navy Unmanned Undersea Vehicle (UUV) Master Plan.

U.S. Department of the Navy, 2013: U.S. Navy Information Dominance Roadmap 2013–2028.

Wenz, G. M., 1962: Acoustic Ambient Noise in the Ocean: Spectra and Sources. *J. Acoust. Soc. Am.*, **34(12)**, 1936-1956.

INITIAL DISTRIBUTION LIST

1. Defense Technical Information Center
   Ft. Belvoir, Virginia

2. Dudley Knox Library
   Naval Postgraduate School
   Monterey, California